UNIVERSITY OF TURKISH AERNAUTICAL ASSOCIATION

INSTITUTE OF SCIENCE AND TECHNOLOGY

INVESTIGATION OF THE FORMABILITY OF THE ADVANCED METAL ALLOY BY HYDROMECHANICAL DEEP DRAWING PROCESS

Master Thesis

Husam Riyad Abdullateef AL-kARAWI

1406080025

IN PARTIAL FULFILLMENT OF THE REQUIREMENTS FOR THE DEGREE OF MASTER OF SCIENCE IN MECHANICAL ENGINEERINGL/PRODUCTION

Supervisor	**Prof. Dr. Ali Çoban**
Co-Supervisor	**Assist. Prof. Dr. Mevlüt Türköz**

Approval of the thesis:

Investigation of the formability of the advanced metal alloy by hydro-mechanical deep drawing process

Hussam Riyad Abdulateef Al-karawi, having student number 1406080025 and enrolled in the Master Program in mechanical engineering / production at the University of Turkish Aeronautical Association, after meeting all of the required conditions contained in the related regulations, has successfully accomplished, in front of the jury, the presentation of the thesis prepared with the title of: "**Investigation of the formability of the advanced metal alloy by hydro-mechanical deep drawing process**".

Prof. Dr. Ali Çoban

Supervisor, Head of department, industrial engineering

Assist. Prof. Dr. Mevlüt Türköz

Co-Supervisor, Mechanical engineering department

Selçuk University

Examining Committee Members:

Assist. Prof. Dr. Hande YAVUZ
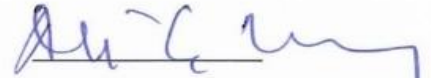
Mechanical Engineering Department, THKU

Prof. Dr. Ali Çoban

Head of department, industrial engineering, THKU

Assoc. Prof. Dr. Murat Demiral

Mechanical Engineering Department,

Çankaya University

Date   04/01/2018

i

I hereby declare that all information in this document has been obtained and presented in accordance with academic rules and ethical conduct. I also declare that, as required by these rules and conduct, I have fully cited and referenced all material and results that are not original to this work.

Name, Last Name: Husam Al - karawi

Signature   :

ABSTRACT

INVESTIGATION OF THE FORMABILITY OF THE ADVANCED METAL ALLOY BY HYDROMECHANICAL DEEP DRAWING PROCESS

Husam Al-KARAWI

M. S., Department of Mechanical Engineering/Production

Supervisor: .... Prof. Dr. Ali Çoban

Co-Supervisor: .... Assist. Prof. Dr. Mevlüt Türköz

January 2018, 80 pages

Hydro-mechanical deep drawing (HDD) is one of a new manufacturing technologies. Low product manufacturing costs, high drawing ratios, high dimensional accuracy, a short production cycle time, high surface finishing, and other advantages have been some of the results of this process. This thesis aims to understand the formability of advanced metal sheets (especially Ti-6Al-4V alloy of thickness 1 mm) at room temperature by using this new process. This is a new study that has not hitherto been performed. This research was conducted both numerically and experimentally.

The process parameters were investigated in simulations. The optimum fluid pressure and blank holder force profiles were especially determined for two forming radii, namely 5 mm and 8 mm. By using these profiles, it was predicted that the (LDR) of the material was 2.4 with the forming radius of 5 mm and 2.2 with the forming radius of 8 mm. It is reported in the literature that the drawing of this alloy is difficult to form below 150°C, but between 150°C and 400°C, the drawing ratio is 1.8 and it becomes easy to form. Although it was predicted in the simulations that the material would form successfully with the HDD process, by using the determined optimal parameters in the

experiments, the material could not be successfully formed. Thus, while it was estimated that the material would be successfully formed with the optimum parameters determined in the simulations, it was found that these parameters did not give a successful forming result in the experimental work.

ÖZET

**HİDROMEKANİK DERİN ÇEKME İŞLEMİ İLE İLERİ ALAŞIMININ
ŞEKİLLENEBİLİRLİĞİNİN ARAŞTIRILMASI**

Husam Al-KARAWI

M.S., Department of Mechanical Engineering\Production

Supervisor …………………….   Prof. Dr. Ali Çoban

Co-Supervisor …….   Assist. Prof. Dr. Mevlüt Türköz

Ocak 2018, 80 sayfa

Hidro-mekanik derin çekme işlemi bu yeni üretim teknolojilerinden biridir. Düşük ürün üretim maliyeti, yüksek çekme oranı, yüksek boyut hassasiyeti, kısa üretim çevrim zamanı, yüksek yüzey işleme ve diğer avantajlar bu süreçten elde edilmiştir. Hidro-mekanik derin çekme işlemi, oda sıcaklığında (Ti-6Al-4V) levha alaşımlı bardakların üretiminde kullanılmıştır. Bu bardağı oluşturmak için iyi bir parametre ve durum bu çalışmanın amacı olmuştur. 1 mm kalınlığındaki (Ti-6Al-4V) alaşım kullanılmıştır. Sayısal ve deneysel çalışma kullanılmıştır. (Ti-6Al-4V) alaşımın Hidro-mekanik derin çekme işlemi sayısal ve deneysel olarak incelenmiştir. İşlem parametreleri simülasyon ile incelenmiştir. Özellikle optimum akışkan basıncı ve pot çemberi kuvvet profilleri, iki şekillendirme yarıçapı (5, 8) mm. için belirlenmiştir. Bu profilleri kullanarak malzemenin Sınırlı Çekim Oranı, 5mm şekillendirme yarı çapı ile birlikte 2.4 olarak ve 8 mm şekillendirme yarı çapı ile birlikte 2.2 olarak öngörülmüştür. Literatürde bu alaşımın çekilmesinin 150 C 'ye kadar oluşmasının zor olduğu ve çekim oranının 400 C' de 1.8 'e ulaştığı belirtilmiştir. Simülasyonlarda Hidro-mekanik derin çekme işlemi ile malzeme

başarılı bir şekilde oluşturulmasına rağmen, deneylerde belirtilen optimal değerler kullanılarak malzeme başarılı bir şekilde biçimlendirilememiştir. Böylece, simülasyonlarda belirtilen optimum parametrelerle malzemenin başarılı bir şekilde oluşturulabileceği tahmin edilirken, bu parametrelerin deneysel çalışmada başarılı bir şekillendirme sonucu vermediği bulunmuştur.

Anahtar Sözcükler: Hidro-Mekanik Derin Çekme ,Ti-6Al-4V Titanyum Alaşım , Sınırlı Çekme Oranı, Şekillenebilirlik, Sac Metal / Levha, Sonlu Elemanlar Metodu.

ACKNOWLEDGMENTS

I would like to express my special thanks and gratitude to my supervisor Prof. Dr. Ali Çoban and co-supervisor Assist. Prof. Dr. Mevlüt Türköz for their guidance, motivation and patience.

A special thanks to my family. Words cannot express how grateful I am to my mother, father, brothers, wife and children for all of the sacrifices that they have made on my behalf. Their prayers for me have been what sustained me thus far.

This thesis would especially not have been possible without the great support of my mother and my wife. Nor would it have been possible without the great support of my uncle and friends.

January 2018   Hussam Riyad Abdulateef Al-KARAWI

TABLE OF CONTENTS

LAST OF FIGURES

LIST OF TABLES

LIST OF ABBREVIATIONS

F_0	Initial force
L_1	Length after changing
L_0	Original length
ΔL	Change in length
A_0	Initial area
A_1	Area after changing
V_0	Original volume
V_1	Volume after changing
σ_0	Engineering stress
ϵ_0	Engineering strain
σ_t	True stress
ϵ_t	True strain
σ_Y	Yield stress
σ_{UTS}	Ultimate tensile stress
HDD	Hydro-mechanical deep drawing
BH	Blank holder
B	Blank
F	Force
{F}	Force vector
{k}	Stiffness matrix
{u}	Displacement vector
F_B	Bending force

F_{DB}	Force draw bed
F_{id}	Ideal force
$D_{B.out}$	Outer diameter of blank
D_P	Punch diameter
D_{BH}	Blank holder diameter
D_s	Seal diameter
t	Blank thickness
σ_{mf}	Medium flow stress
σ_{Bfo}	Flow stress at outer edge of blank
σ_{BfDi}	Flow stress at inner drawing opening
P_c	Chamber pressure or cavity pressure
$\beta_{\circ}$	Drawing ratio
P_{HB}	Blank holder pressure
PC	Personal computer
PLC	Programmable Logic Control
r	Radius of measured to mid plane
θ	Bend angle
z	Distance of an element from the mid plane
$\in_x$	True strain in x-ax

CHAPTER ONE

INTRODUCTION

1.1 Back Ground

Sheet forming is very important process, it entered to manufacturing many parts in automotive and air craft body structure. Low density metal and modern manufacturing processes used instead of high density metal and traditional manufacturing processes is goal for any company to reduced cost. In this time; Aluminum, magnesium, titanium alloys widely used in cars and aircraft bodies instead of steel alloys and other have alloy because it has low density. Light alloys metal make structure lightest. New manufacturing processes also have been used to manufacturing parts. One of these new process hydro-mechanical deep drawing process (Fig. 1).hydro-mechanical deep drawing has been used to produce many main parts enter to manufacture automotive and aircraft bodies (Fig. 2). Hydro-mechanical deep drawing is a new technology to form parts from sheets. It is resulting from hydroforming technology and traditional deep drawing or it unite between traditional deep drawing technology and hydroforming technology [1].

In fact, there are many types of hydroforming process, such as hydrodynamic deep drawing, hydro-mechanical deep drawing, aqua-draw deep drawing, fluid former, drawing with counter pressure and others [1, 2].
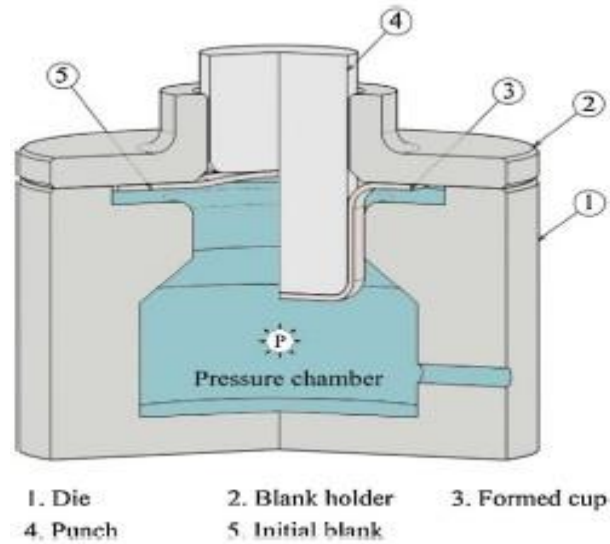
Figure 1: Hydro- mechanical deep drawing die general view [23]

| 1. Die | 2. Blank holder | 3. Formed cup |
| 4. Punch | 5. Initial blank | |

A
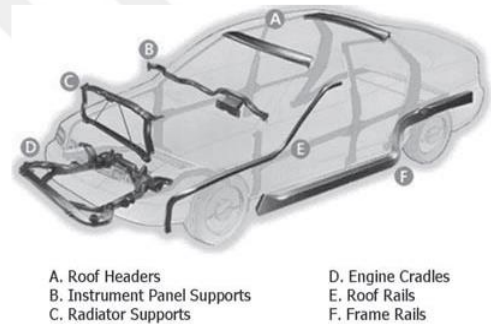
B

Figure 2: (A) Hub using in aircraft engine manufacturing by hydroforming process **(B)** Parts using in car body manufacturing by hydroforming process [21]

However, the development of the hydro-mechanical deep drawing process passed through various periods time one-hundred years ago especially after the Second World War. In Japan, the first investigation to produce press forming with hydraulics occurred around 1955. After then, Prof. Y. Kasuga et al. utilized hydraulic pressure (Fig. 3) produced by the permeation of a punch in a die cavity, the results of which were noted from 1958 to 1964. [3]
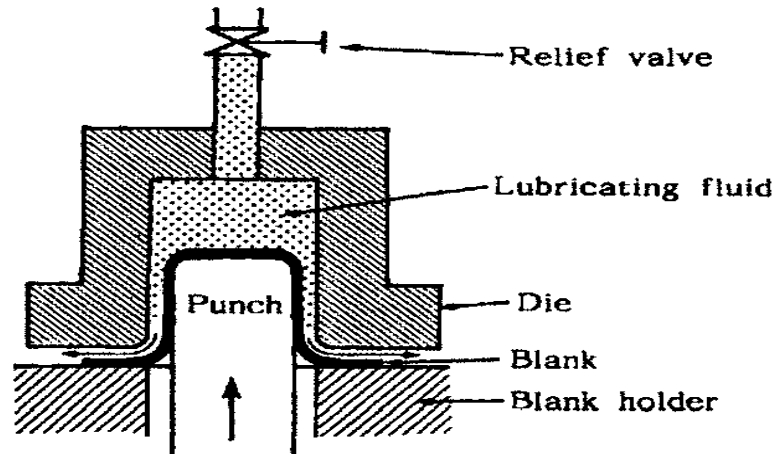
Figure 3: Mechanism of hydro-mechanical deep drawing in japan between (1958-1964) [3].

In 1975 and the years afterwards, Japanese researchers began to work on the hydraulic counter-pressure fluid-forming process. The radial-pressure deep drawing method was proposed during this period. In Germany, researchers in this field began their work in the 1950s. To prevent oil leakage between the die and the blank, researchers placed a seal-ring on the female die face. In the Netherlands, researchers started work on the Daalderop method in 1961. Chinese scientists worked on this technology later in 1997 [1]. In recent years, many countries, such as the USA, France, China and others, have rapidly progressed in this technology. Researchers have made efforts to develop this process because of the great benefits of this process when compared with the traditional deep drawing. These developments lead to more advantages. Low tool costs, higher dimensional accuracy, shorter cycle times, high drawing ratios, high surface finishing, complex shapes, etc. have been some of the results of this method. All these properties of products manufactured in this manner became more competitive relatively to other manufacturing processes, mainly for low-volume production, but also in some cases for high-volume production. In the automotive manufacturing industry, there is a need for low-volume production of body components.

As mentioned earlier, one of the main reasons for the reduction of fuel consumption in cars and aircraft is the replacement of heavy parts in car and aircraft structures with light parts while keeping their strength. Light metals and their alloys are

appropriate and important choices in automotive and aircraft structures. Originally, only aluminum and magnesium were used. Afterwards, other elements in the periodic table were included. Titanium was also included in this group. Density is the main element that distinguishes metals in the periodic table. In the periodic table, we can read the relative densities ranging from 1.7 to 4.5 for magnesium and titanium (light metals), respectively, which contrast with 7.9 to 8.9 for iron and copper (heavy metals), respectively. These differences between the densities were employed to reduce structural weight. For example, the stiffness of a simple rectangular beam is directly proportional to the product of the elastic modulus and the cube of the thickness. An iron (or steel) beam weighing 10 kg will have the same stiffness as a titanium beam of equal width and length but weighing 7 kg, weighing 4.9 kg for aluminum, 3.8 kg for magnesium, and only 2.2 kg for beryllium [4].

Titanium (with its alloys) is one of the famous metals belonging to the light metal group. Titanium is the ninth most plentiful element on Earth and titanium alloys are the fourth most-used structural materials. Titanium is a low-density element (approximately 60% the density of steel and super alloys) that can be strengthened greatly by alloying and deformation processing. Titanium was discovered in 1790 as an element in the UK and called *titan* by German scientists in 1795 [7]. Only in the second half of the 20th century did metallic titanium gain strategic value. Titanium has interesting mechanical and physical properties and its alloys have good characteristics. As a result, titanium is defined as a metal having commercial importance. In fact, in the 1930s in the United States, Dr. Wilhelm J. Kroll discovered the first method to produced titanium as a tetrachloride (TiCl$_4$). Dr. Kroll and other scientists continued to improve methods of reduction of titanium during the 1940s [5]. In 1949, Douglas Aircraft became the first company in the United States to use titanium in aircraft, and in 1948 in the UK, the first use for titanium in aircraft and military fields we recorded. In 1952, titanium began to be used in the industrial field in Japan. The U.S. government was interested in developing the science and technology of titanium and its alloys for this goal as the government invested large amounts of money in this field. As a result of these investments, the development of titanium alloys progressed quickly from about 1948 to 1954. During these years, scientists

exploited the effects of aluminum additives and produced the (α+β) Ti-6Al-4V alloy, after which the same group discovered the β alloy Ti-13V-11Cr-3Al, which is a high-strength heat-treatable alloy [5]. After this period, most titanium alloys were used in military applications, such as the SR71 type aircraft (Fig. 4) and gas turbine engines (Fig. 5) [7]

Figure 4: SR71 aircraft: first use of beta alloys in aerospace structures [7]
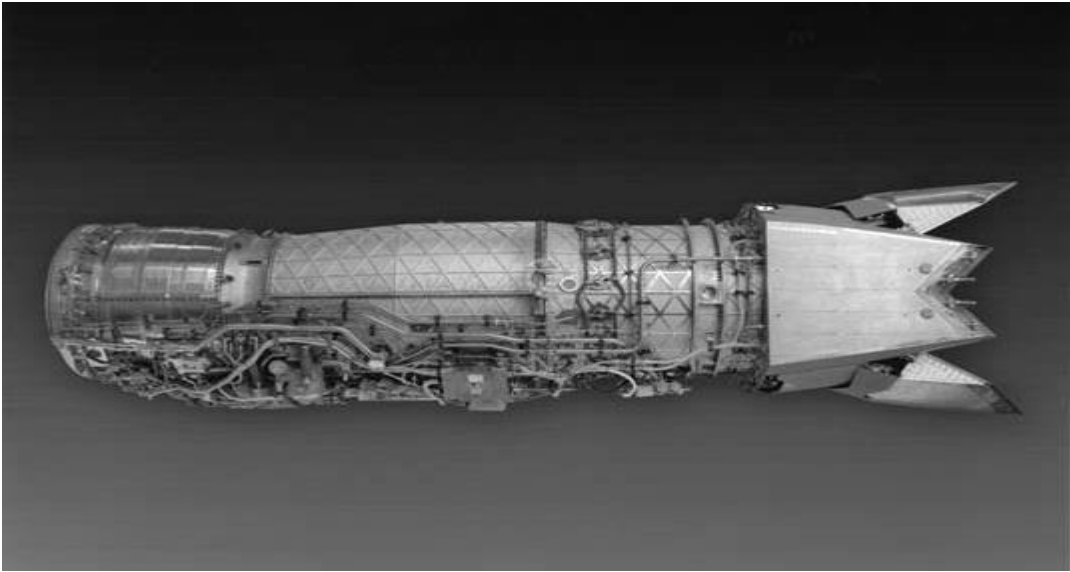
Figure 5: Engine by Pratt & Whitney powering the F22 Raptor aircraft [7]

Today, titanium alloys are very important alloys in industry because of their astonishing properties, most important of which are their light weight, high specific strength, corrosion resistance, protective oxide layer, their ready formability and machinability. Moreover, titanium alloys can be forged or wrought by standard techniques and they are castable. The titanium microstructure at room temperature consists of α. However, above a temperature of 882°C, the alpha (α) phase changes to the beta (β) phase (Fig. 6 and 7) [6-7].
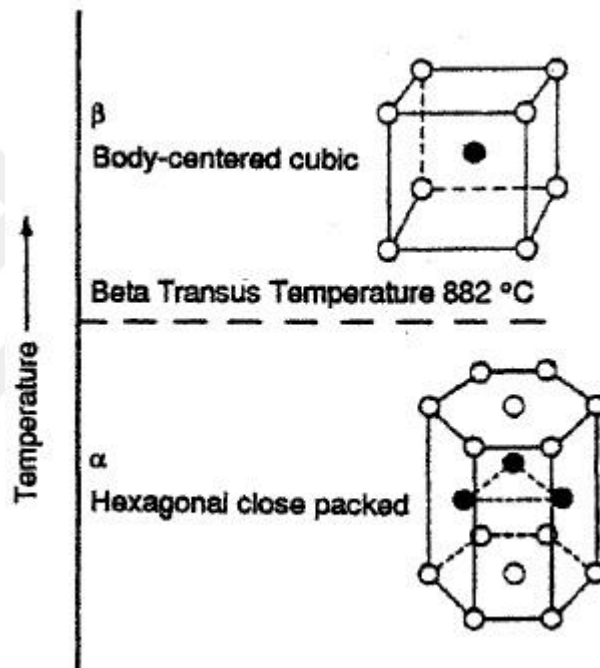
Figure 6: Show changing phase from alpha to beta with increase temperature [5]
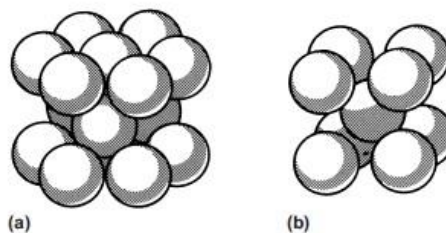
Figure 7: Showing the two crystal structures for titanium (a) alpha, (b) beta [7]

Titanium alloys are classified into four types according to alloy microstructure. These types are the (α) alloys, (β) alloys, (α+β) alloys and intermetallic (Ti_xAl) [5]. The Ti-6Al-4V alloy is one of the (α+β) alloys. Ti-6Al-4V alloy comprises approximately 45% of the total weight of all titanium alloys shipped [7]. The importance of this alloy is due to its properties, such as its ability to resist high temperatures, its good corrosion resistance, high tensile strength, and its resistance fatigue strength, low modulus of elasticity, low density, and high hardness. These properties see this alloy being used widely in many applications, especially in the automotive and aircraft industry. In the automotive field, the alloy is used by the most famous companies in the manufacturing of engine parts (Table 1), including connecting rods (Fig. 8), turbo charger wheels, engine valves (Fig. 9), exhaust systems, and suspension springs (Table 1). In the field of aircraft manufacturing, most internal engine parts were made from titanium alloys, especially Ti-6Al-4V alloy. Moreover, this alloy was a component material in other important parts of aircraft body structure. On the other hand, this alloy has disadvantages such as the spring back phenomenon, high cost and poor formability in cold conditions.

Table 1: Showing some famous companies used (Ti-6Al-4V) alloy in engine. [24]

No.	Company name	Parts name
1	Ferrari (1992)	All engine connection rods (Ti-6Al-4V)
2	Bugatti (2005)	All engine connection rods in Veyron 16.1made from (Ti-6Al-4V)
3	GM	All valves made in engine made from(Ti-6Al-4V)`

Figure 8: Connection rods [24]

Figure 9: Engine valves [24]

Therefore, this alloy is difficult to form in a traditional forming process such as traditional deep drawing and press forming. A numerical study is very beneficial before work any experimental work. In sheet metal forming, modelling and simulation can be utilized for many purposes, such as to forecast material flow, to analyze stress-strain distribution as well as temperature distribution in order to determine the effective force to form parts, to predict possible sources of defects and failures, to improve the quality of parts and to reduce manufacturing costs. The simulation process has been occurring in two time periods, the first of which was before 1990. During this time, the different attempts and trials were mainly dependent on approaches, such as expert systems and understanding based methods. The second period started in 1990 at which time a huge effort had been expended on making finite element (simulation) technology easily accessible for industry to use in common complex industrial problems [25].

1.2 Aim of This Thesis

Engineering parts produced by a hydro-mechanical deep drawing process have good physical properties due to the use of soft female dies (hydro properties) instead of hard female dies used in traditional deep drawing. Pressurized fluid in a female die in hydro-mechanical deep drawing process produces parts with astounding properties in contrast to parts produced by traditional deep drawing. Therefore, products manufactured with the hydro-mechanical deep drawing method have good specifications which are due to many reasons. The first reason, the products can be produced from effective pressurized hydraulic fluid in a cavity. This compressed hydraulic fluid in the cavity reduces fractures and prevents wrinkle effects and leads to obtaining a higher drawing ratio. In addition to the forming steps, number and sizing tools (only the punch is used to produce parts), the t sizing operation is reduced, and a high product quality and size is obtained from effective pressurized hydraulic fluid. All these characteristics make the product cheaper. The second reason is that they are produced from forces generated during forming time via the process. The forming force between the punch and the blank and the lubrication effect of the liquid between the blank and the drawing ring lead to a reduction in damage between all parts. High surface finishing, high dimensional accuracy and less wear in the die are also other benefits. The third reason is the friction holding effect from which a light local

thinning and a uniform thickness distribution can be produced. Complex shapes and materials that are not suitable for intermediate heat treatment can be produced, in addition to other advantages [1]. The main motivation of this study is the advancement of science and the selective enhancement of Ti-6Al-4V sheet alloy for improved formability, and finding the optimal parameters for forming by using the hydro-mechanical deep drawing process at room temperature. This was a great challenge as the Ti-6Al-4V alloy exhibits a high degree of spring back and strain hardening in cold forming. These properties normally increase tensile and yield strengths as well as a slight drop in ductility [7]. Other studies have suggested that forming this alloy in hot working or superplastic forming produces good forming parameters. Therefore, the traditional deep drawing of a Ti-6Al-4V alloy sheet largely has been replaced by superplastic forming.

This study aims to understand Ti-6Al-4V sheet alloy forming behavior at room temperature by using the HDD process, i.e., forming this alloy in cold working. Our goal is to obtaining the optimal parameters to form this alloy and to exploit the advantages of the hydro-mechanical deep drawing process at room temperature to overcome badly forming characteristics of the alloy. Our studies include several stages to achieve the goal of this study. Stage 1 includes a study of the microstructure of the alloy and the effects on the formability of this alloy, after which heat treatments are applied to improve the microstructure of the alloy. To improve its formability, mill annealing is used. Tensile testing is performed before and after heat treatment. The results are discussed to determine the behavior of the alloy. The second stage determines the optimal parameters using the simulation programs SOLIDWORKS, DYNAFORM, LS-DYNA, and ETA POST PROCESSOR. In the third stage, the resulting parameters are taken from the simulation and employed in the experimental work. Finally, we compare the results between the experimental and numerical results.

1.3 Structure of the Thesis

Chapter One presents the history and development of the hydro-mechanical deep drawing process. Titanium and the development and importance of its alloy (Ti-6Al-4V) are also presented in addition to an explanation and aim of this thesis.

Chapter Two is divided into two parts. The first part is a review of other studies on the benefits of the hydro-mechanical deep drawing process to improve light metal formability. The second part is a review of other studies on the benefits of the forming process to form the Ti-6Al-4V alloy and the optimal parameters that needed to be determined to improve formability.

In Chapter Three, we present research on the physical properties of the Ti-6Al-4V alloy, including the heat treatment process applied to the alloy, the effects on its microstructure, tensile tests before and after heat treatment, and the effects of the heat treatment on the physical properties of the alloy. The advantages, principles and forces of the hydro-mechanical deep drawing process are also presented.

Chapter Four presents explanations of the principles, parameters and details of the simulation as well as the tools, methods and machinery being used in the experimental work.

In Chapter Five, we present and discuss the numerical and experimental results for (Ti-6Al-4V) alloy and stainless steel type 304. . In the final part of this chapter, the results of a numerical and experimental study of the manufacture of stainless steel 304 cups have been developed using this method to prove the method (numerical and experimental) study which used to manufacture cups made from (Ti-6Al-4V) alloy is correct and the problem in another place.We also discuss a comparison of the numerical and experimental situations and conclude the thesis with a brief presentation.

CHAPTER TWO

LITERATURE SURVEY

2.1 Introduction

For the high quality of the product produced by this method, and for the good results achieved from using it, many studies have been conducted on the improvement of metal formation conditions using hydro-mechanical deep drawing. In this chapter, we review and summarize these studies. The chapter divided into two parts: The first part reviews the studies which have focused on improving the conditions of formability for light metal alloys through hydro-mechanical deep drawing and achieving the best results. In the second part, we review and summarize the studies pertaining to the improvement of Ti-6Al-4V alloy formability.

2.2 Studies Focusing on the HDD Process

In Part One, we focused on the studies that have benefited from the use of hydro-mechanical deep drawing to improve formability to other alloys. The results of this improvement and the conditions accompanying the work have been summarized here.

Lihui Lang et al. (2007) [8] studied enhancing the aluminum alloy sheet formability type (Al 1050-H0) by using hydro-mechanical deep drawing. The researchers investigated the parameter affecting the quality of the cups, and the methods to improve sheet formability and quality, which was carried out both experimentally and in simulation. They selected the LS-DYNA program to conduct the simulation. For the sheet, they selected one of 1.24 mm thickness, 375-ton Lagan double action, 10-30 mm/s punch

speed, 30 MPa pre-bulging pressure and others parameters as conditions for this experiment. They chose to study improve roundness via a changed drawing ratio and pre-bulging, and improved the wall thickness distribution by changing the drawing ratio value. As a result of this study, they found an agreement between experimental investigation and the simulation. The drawing ratio played an important role in the final results and when the drawing ratio was high, the roundness increased commensurately. When the pre-bulging pressure was higher, the roundness became bad, and due to the radial pressure, the drawing ratio was able to reach a higher limitation and when the drawing ratio was high, the wall thickness started to become thinner.

Lihui Lang et al. (part 1) (2004) [9] studied replacing the deep drawing process with hydro-dynamic deep drawing to form cups made from aluminum alloys due to their bad cold formability in deep drawing by studying the effect of some parameters in enhancing the formability of the aluminum alloy. The parameters studied were the failure modes, the optimal gap between the blank holder and the die, the pre-bulging parameter, the liquid pressure in the cavity and the routine of the liquid pressure in the die. The researchers used A16016–T4 type aluminum alloys with a thickness of 1.15 mm and a 375-ton hydraulic press. As result of this experiment, the maximum drawing ratio reached was 2.46. The researchers classed the fracture into three types: the initial fracture; the middle fracture and the final fracture. Moreover, they classed the wrinkling types as body wrinkling and flange wrinkling. They found the optimal condition to avoid failure, which were a gap between the blank holder and the die ranging from 0.98 to 1.035 times the original thickness of the blank, a maximum pressure in the die cavity equaling 325 bars, a pre-bulging pressure equaling 200 bars and an optimal pre-bulging height of approximately 0.0 mm.

Lihui Lang et al. (part 2) (2004) [10] studied enhancing aluminum alloy type (AL6016-T4 and Al-Mg-Si) formability with 1.15 mm thickness by utilizing hydro-dynamic deep drawing. Experiments and numerical simulations were performed to calculate the optimal parameters. The loading boundary conditions, the effects of sheet anisotropy on the material flow velocity distribution, the stress distribution, the strain

distribution, and the sheet thickness distribution were investigated. A 375-ton Lagan press with a punch speed of 30 mm/s was used in the experiment. As a result of this study, the fluid pressure loaded onto the rim of the blank was ignored and by changing the appropriate friction coefficients, the best parameters were able to be obtained in the simulation depending on the maximum punch force. They found that with sufficient lubrication between the blank and the blank holder, the blank and the die would be useful to develop the sheet drawing ratio. For the other result, they found that when they had kept the friction coefficient larger than one certain value between the blank and the punch, the forming process continued without fractures. The blank flange tended to wrinkle because the liquid would be pushed into the seam between the blank and the blank holder. This defect would need to be removed before the flange could be pulled into the die cavity; otherwise, body wrinkling would form.

Wei Liu et al. (2014) [11] studied one of the main defects which occur in the sidewall for a curved surface part. Wrinkling in a sidewall of a curved surface part is a major problem which occurs during traditional deep drawing processes. Wrinkling has a major effect on surface quality and service performance. This group studied overcoming this defect by replacing the traditional deep drawing process with a hydro-mechanical deep drawing process. The pre-bulging phenomenon in the hydro-mechanical deep drawing process was used to control the wrinkles on the curved surface part, and they also benefited from a soft die (female die) in the hydro-mechanical deep drawing to control the wrinkles. Moreover, they investigated this in experiments and in numerical simulations with the LS-DYAN program. As a result of this study, wrinkling occurred in the unsupported region. The chamber pressure was insufficient to avoid wrinkles on parts of the surface. The chamber pressure could be used to reduce the wrinkles only; however, a high chamber pressure led to cracks on the unsupported region caused by higher tension stress. Pre-bulging pressure in the hydro-mechanical deep drawing process can be utilized to remove wrinkle by reducing the tangential compressive stress on unsupported region, and increasing the area of sheet attached to the punch surface. Therefore, higher pre-bulging pressure can increase tangential plastic strain of an unsupported region and the

pre-bulging results of the biaxial tension effect which results in a greater ability to avoid wrinkles of the blank on unsupported regions.

E. Ceretti et al. (2005) [12] studied the hydro-mechanical deep drawing process parameters in a numerical study. They improved the process conditions (optimal conditions) in a simulation. They did so by studying the influence of geometrical features of a pressure chamber in terms of the gap with the punch together with the main process parameters, such as counter-pressure and Blank Holder Force (BHF). As result of this study, if counter pressure increased very quickly in the first part of the process, it would lead to minimum friction between the blank and the die entrance radius. The blank holder force can be determined by the pressure path. The other result of this study was that the part wall thickness was found to decrease in the first half of the simulation, after which it remains constant. Evaluating the success of the simulation depends on the thinning and wrinkles of the final results. They performed the simulation by using the PAM STAMP 2000 program with the Aquadraw program.

Takeshi Uemori et al. (2017) [31] studied enhancing the high strength steel sheet [HSSs] formability .stretch bending process has been used to reach of this goal. 2 mm and 8 mm punch radius have been used. Fracture limits in stretch bending and using two no dimensional parameters [limited wall stretch ($L/L_\circ$) & bending radius (t/r)] have been studied .as a result of this study punch radius has a great effect on limited forming height the study review here to know bending radius effective due to in this thesis we used this parameter to enhance (Ti-6Al-4V) alloy formability.

2.3 Studies Focus on Enhancing Ti-6Al-4V Formability

In Part Two, we focus on attempts to improve the formability of a Ti-6Al-4V alloy sheet using other processes or by using a heat treatment process. The reason for writing a summary of improving alloy formability via other processes other than hydro-mechanical deep drawing is due to the fact that no study dealing with this subject has been found. This is interesting and at the same time difficult. Studies that have done so include the following:

Liu Wanying et al. (2017) [13] studied the influence, solution and aging treatment on the microstructural and mechanical properties of the Ti-6Al-4V (grade 5) alloy. The researchers discussed the relationship between the microstructure, impact fracture characteristics and mechanical properties by changing heat treatment conditions. A metallurgical microscope, tensile mechanical test, X-ray diffraction (XRD) test and an environment scanning electron microscope were used to analyze their results. A 6 mm thick Ti-6Al-4V alloy sheet was in their experiment. A solution and aging treatment was used in their study to reduce or eliminate the α-phase of the continuous grain boundary and create a more stable β-phase and make the β-phase more metastable. This leads to a significant improvement in tensile and fatigue strength. As a result of this study, they found that heating this alloy to 960°C for one hour and cooling it in water and heating again, but to 500°C for 4 hours and cooling it by air was the best condition to improve the mechanical properties to form such alloy sheets.

Ossama Mamdouh Badr et al. (2004) [14] studied enhancing Ti-6Al-4V formability at room temperature by changing manufacturing methods (from bending to rolling). To reduce costs they did not enhance it via hot forming. They studied the spring back phenomenon in this alloy and how to avoid it or reduce it. They also studied the forming limit diagram (FLD). To do so, they used a 2 mm alloy sheet which was manufactured by cold rolling with mill annealing at 850°C. They performed tensile tests to determine the physical properties and drew true strain-stress curves. This study was performed experimentally and numerically. As a result of this study, the showed that this

alloy has very limited formability at room temperature and produced sudden fracture without the growth of a distinct neck. The phenomenon of spring back occurs very clearly in this alloy. Due to these reasons and others, they suggested forming this alloy at room temperature by using roll forming instead of bending, stamping or deep drawing processes.

J. Adamus et al. (2012) [15] attempted to enhance the formability of titanium alloy sheets, especially Ti-6Al-4V alloy, by using the flexible tool shown in (Fig. 10). The study was performed experimentally and in numerical form by using the ADINA System for the numerical study. The researchers changed many parameters to produce higher material deformation without risk of fracture. They formed a cup thickness of 0.8 mm and a diameter of 48 mm. As result of this study, they have had good titanium alloy sheet formability between the fix punch and rubber bed (due to the large deformation of the rubber pad), in addition to producing a good surface finish.
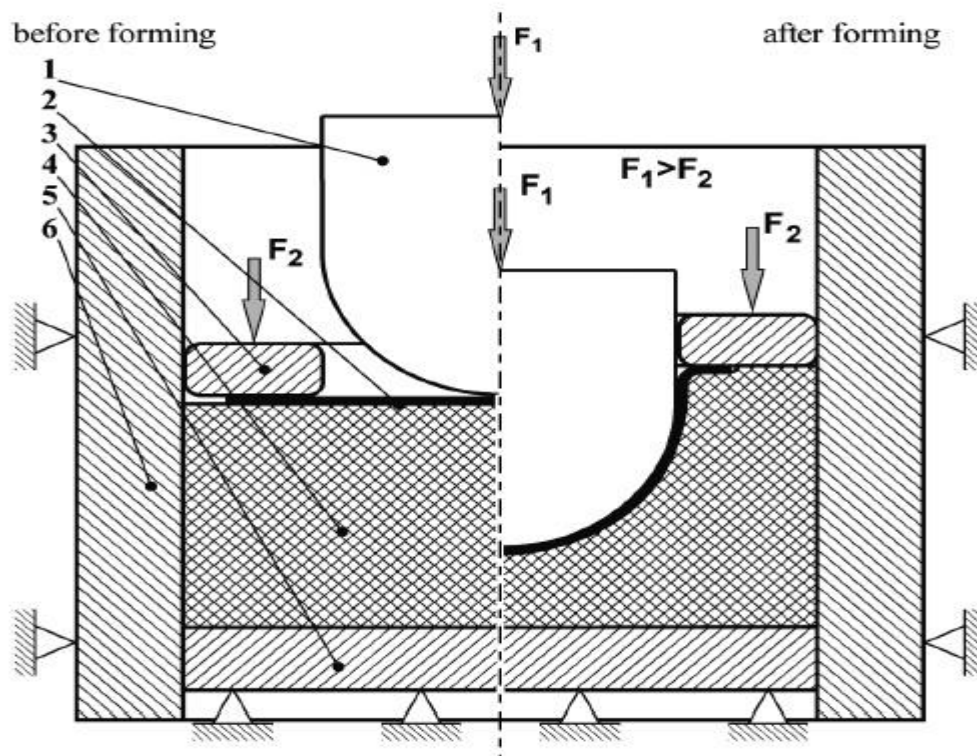
Figure 10: Showing special tool with rubber bed [15]

(1)Punch (2) blank (3) flexible pad (4) rubber bed (5) working tube chamber (6) double action press

16

Tuoyang Zhang et al. (2014) [16] studied enhancing Ti-6Al-4V alloy formability by exploiting the superplastic phenomenon and studying its effects. A 1.4 mm thick Ti-6Al-4V alloy sheet was used by the researchers who conducted tensile tests and at various temperatures, including room temperature, to determine the physical properties for the alloy. They selected 700°C, 750°C, 800°C, and 850°C as experimental temperatures for the hot tensile test. The 800°C temperature produced maximum elongation (825%) in the tensile test and at this temperature the deformation activation energy was similar to the grain boundary self-diffusion energy. The deformation mechanism was mainly grain-boundary sliding; i.e., it was the optimal temperature for this alloy in a superplastic state. The Ti-6Al-4V alloy had a typical α+β microstructure such that the size of the alpha (α) phase grain was fine and homogeneous. This alpha case was very brittle and tended to cause cracking. The alpha (α) phase could reduce Ti-6Al-4V performance and fatigue properties [17], but the beta (β) phase grains were distributed uniformly between the grain boundaries. After heating, the fine grain size, narrow grain size distribution, low grain aspect ratio and high volume part of the β phase was able to lead to large elongations.

F. Djavanroodi et al. (2010) [18] studied the enhancement of titanium alloy (Ti-6Al-4V) and aluminum alloy (Al6061-T6) via a hydro-forming deep drawing process assisted by a floating disc (Fig. 11). The fracture mode, strain distribution and forming limited diagram were also studied. They conducted their research in experimental and numerical form by using the ABAQUS/Standard. As a result of their study, Ti-6Al-4V alloy and Al6016-T6 alloy sheets were successfully formed when utilizing a hydroforming deep drawing die assisted by a floating disc. Due to the simplification of the tools and processes, there were benefits, such as a decrease in punch force and cost. From the tensile test, the optimum values of strain-hardening were found to be *n* equaling 0.145 and 3.02, and the strain-rate sensitivity *r* equaling 0.17 and 0.57.
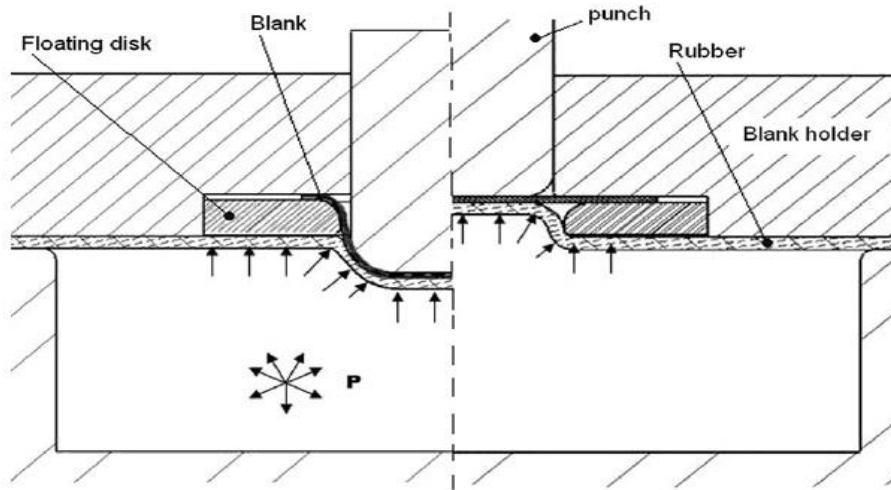
Figure 11: Showing hydroforming deep drawing assisted by floating disc [18].

Nitin Kotkundea et al. (2015) [19] studied the enhancement of Ti-6Al-4V alloy formability by using deep drawing and stretching processes under warm conditions. Thickness distribution, earing profile, dome height and the forming limit diagram were studied in experimental and numerical forms. Cups formed with 0.9 mm thick sheets were used. A warm tensile test (heating to 400°C) with three angles of rolling direction (0°, 45°, 90°) from this alloy were performed to calculate the physical properties. As result of this study, the maximum LDR of 1.86 was obtained. All parameter results which were calculated in experimental and numerical forms were similar with error percentages of 3.33%. For the Barlat 2000, the yield criterion was studied and the results were very good and suited to predicting the yielding behavior of Ti-6Al-4V alloy in warm conditions.

Nitin Kotkunde et al. (2014) [26] studied the enhancement of Ti-6Al-4V alloy sheet formability by using a traditional deep drawing process under warm conditions. The study was performed in a temperature range between room temperature and 400°C on a sheet thickness of 0.9 mm. A simulation program was used to study parameters before the experimental work. This study showed that Ti–6Al–4V alloy is difficult to draw at temperatures between room temperature and 150°C. Above this temperature range to 400°C, the drawing ratio reached 1.8. The thickness distribution at the optimum setting for experimentation shows good agreement with that of the simulated deep drawn cup.

18

CHAPTER THREE

MATERIAL AND METHOD

3.1 Introduction

In this chapter, the characteristics of the titanium alloy type (Ti-6Al-4V) from the grade 5 groups are discussed in addition to a discussion of the effect of the percentage of the elements in the Ti-6Al-4V alloy. For the purpose of improving the specifications of the Ti-6Al-4V alloy, heat treatment was applied. Mill annealing was used as a solution to enhance the alloy microstructure to obtain good physical properties. The effects of mill annealing before and after the process on the microstructure are discussed. For the purpose of knowing the mechanical properties of the Ti-6Al-4V alloy, a tensile test was performed, which was carried out before and after the heat treatment to determine the alloy properties in the two cases. Knowing the physical properties in both cases gives an understanding of the effect of the heat treatment on it. The final part of the chapter is dedicated to the hydro-mechanical deep drawing process. The working mechanism is explained and the main parts that must be provided to complete the process are mentioned in addition to a discussion and explanation of the main forces influencing the formation process.

3.2 (Ti-6Al-4V) Alloy Properties

As mentioned in the introduction, a titanium alloy (Ti-6Al-4V) belonging to the grade 5 family sheet was used in this study. This alloy comprises 50 percent of global consumption of titanium alloys. It is one of the alpha-beta alloys and it is used in many applications. The chemical composition of this alloy comprises different percentages of elements (Table 2).

Table 2: Showing elements percentage in Ti-6AL-4V alloy [4].

grade	Al	V	O	Fe	C	H	N	Ti
5	5.5 – 6.75	3.5–4.5	≤0.20	≤0.30	≤0.08	≤0.015	≤0.05	balance

The characteristics of this alloy are dependent on the percentage of elements. According to the use of the alloy, the percentage of aluminum in this alloy ranges from 5.5% to 6.75%. For example; the aluminum ratio was limited to 7.0% due to the ductility of the resulting alloy decreasing to such an extent that the forming and drawing qualities and the vanadium percentage range from 3.5% to 4.5%. The ratio of vanadium in the alloy indicates the weldability of the alloy. This percentage depends on the use of this alloy such that if we need weldability to override strength and ductility, the vanadium content should be limited to 4%. Conversely, when weldability is not important, the vanadium content can increase to 6% for higher tensile strength. The alloy name Ti−6Al−4V is the nominal composition only [4]. Other elements affect the microstructure of this alloy. For example, hydrogen makes the beta phase more stable. When the temperature lowers the β transus temperature line, oxygen, nitrogen and carbon make the α phase more stable and alloying elements have an effect on the stability or instability of the beta phase [17].

3.2.1 Heat Treatment

Ti-6Al-4V consists of two phases: the α phase (which is Body Centered Cubic (BCC)) and the β phase (which is Hexagonal Close Packed (HCP)), which is also allotropic. Because of the crystalline structure, there is a greater amount of beta phase than alpha phase. Titanium alloy phases change at varying temperatures according to alloying element percentages and concentrations. The α phase changes to the β phase with an increase in the temperature at a temperature known as the β transus line. In this alloy, the phase transformation occurs at 800°C due to the percentages of alloying elements (Fig. 12).
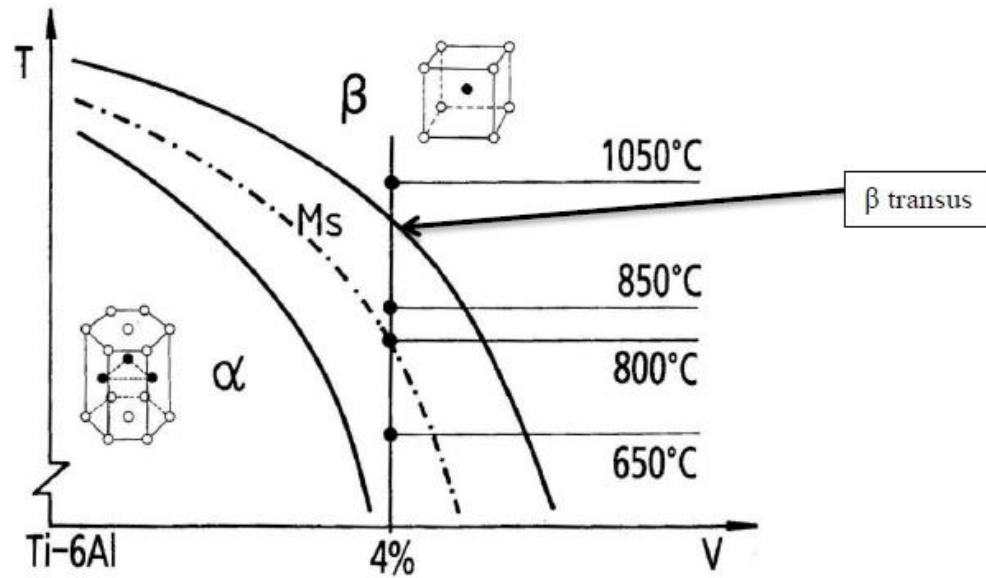
Figure 12: Phase diagram of Ti-6Al-4V with unit cell [17].

The β transus temperature line is affected directly by the alloying component content that acts as α or β in relative stability. Hydrogen makes the β phase more stable when the temperature falls to the β transus temperature line while oxygen, nitrogen and carbon make the α phase more stable. The alloying elements have an effect on the stability or instability of the β phase, whereas the effect of the microstructure of the alloying elements have a higher β phase than titanium helping to fix the β phase. Generally, tantalum, molybdenum, niobium, and vanadium make the β phase more stable [17].

A Ti-6Al-4V alloy sheet has poor forming properties at room temperature. It exhibits a high degree of spring back in cold forming, so heat treatment is performed to enhance its physical properties. Mill annealing is good method to enhance alloy formability by changing the microstructure of this alloy (Fig. 13). Enhancing the mechanical properties, such as yield strength and ultimate strength, are the goal of heat treatment, which includes a reduction of residual stresses developed during rolling (stress relieving). In this study, we used mill annealing, which served primarily to increase toughness, ductility at room temperature, dimensional and thermal stability. At times, creep resistance had been considered a process [7].
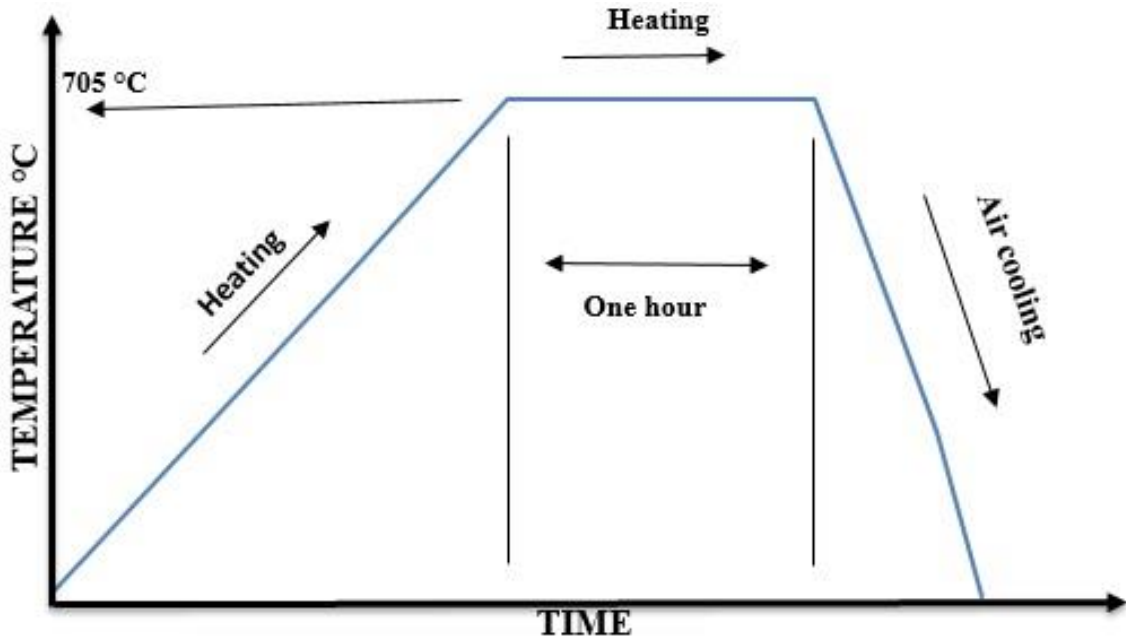
Figure 13: Showing mill annealing procedures.

The heat treatment process was performed using a PROTHERM-PLF 130/12 electric furnace in a laboratory at Selçuk University (Fig. 14). Heat treatment was applied to the specimens for 1 hour at 705°C. Upon completion of that hour, the oven was switched off and the door of the furnace opened to cool the specimens by air (Fig.17 & Fig.18). Good results were obtained from this process. The heat treatment helps to improve the alloy microstructure by increasing and re- augmenting the beta phase in the crystal structure. The difference between the mechanical properties before and after the mill annealing process can be observed in (Tables 4 and table 6). Moreover, a change in the surface color is observed after heat treatment (Fig. 17) due to the interaction of oxygen with the surface and the formation of a layer of alpha (α) phase ranging in thickness from 23.3 to 25.8 [17] (Fig. 18).

Figure 14: Temp. Regulator.

Figure 15: Over view of furnace.

Figure 16: The specimens before heat treatment.

Figure 17: Specimens after mill annealing.

Figure 18: Specimens after heat treatment.
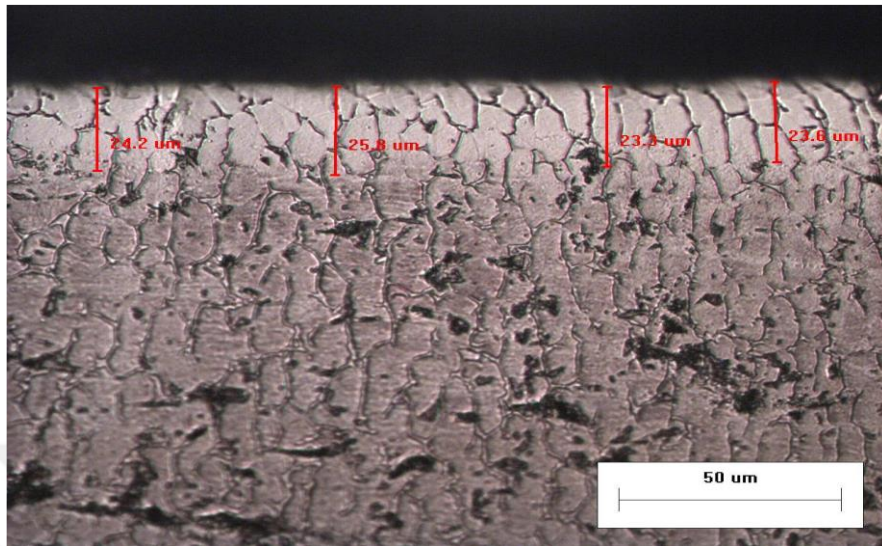
Figure 19: Alpha phase and associated measurements on the surface of an annealed sample of Ti-6Al-4V. [17].

As mentioned previously, the microstructure of this alloy consists of two phases. The main phase is the alpha (α) phase and the beta (β) phase stabilizes along the boundaries of the (α) phase grain. After the mill annealing process, the influence of grain recrystallization and growth occur, which lead to an enhancement of the mechanical properties of yield and ultimate strength (Fig. 20).
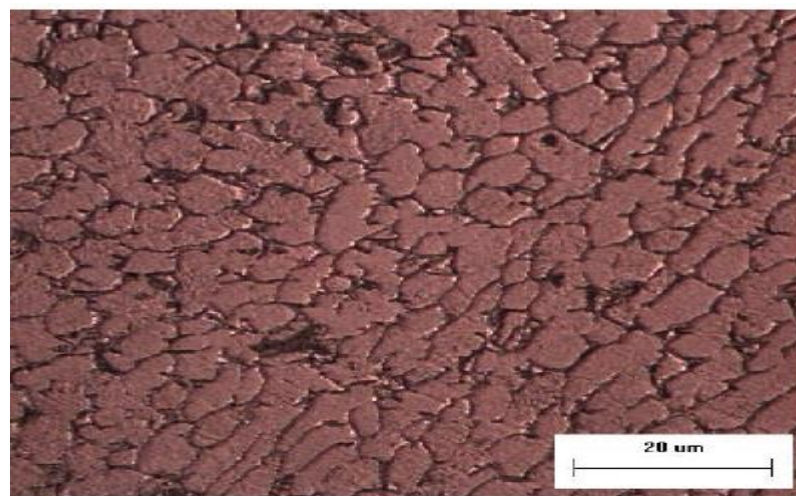
Figure 20: Alpha phase and associated measurements on the surface of an annealed sample of Ti-6Al-4V. [17].

3.2.2 Tensile Test

One of the most shared mechanical stress–strain tests is performed in the tensile test. The tensile test can be used to determine several mechanical properties of materials that are important in design. A specimen is deformed to fracture, with a slowly increasing tensile load that is applied uni-axially along the long axis of a specimen. (Fig. 21) for a standard tensile specimen and for the overall dimensions for a tensile test specimen (Table 3) Many parameters can be determined from a tensile test, such as the Modulus of Elasticity, upper yield strength, lower yield strength, and ultimate tensile strength, percentage elongation after fracture, percentage reduction of area, elastic area and plastic area.
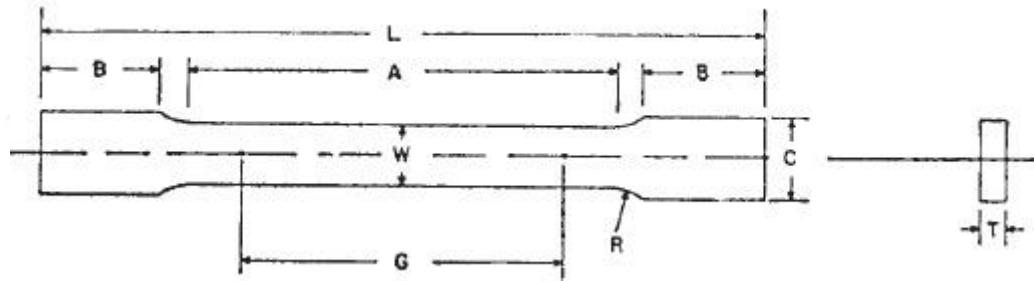
Figure 21: A standard tensile specimen dimensions[27].

Table 3: Overall dimensions for tensile test coupon [27].

Symbol	Description	Dimensions (mm)
G	Gage length	50
W	Width	12.5
t	Thickness	1
R	Radius	12.5
L	Overall length	200
A	Length of reduced section	57
B	Length of grip section	50
C	Width of grip section,	20

After the specimen is installed in the tensile test machine, the machine starts to pull in two opposite directions. A fracture occurs in area G before the other areas in the same specimen. This happens because of engineering stress (σ_0), which is defined by the mathematical relationship:

$$\sigma_\circ = \frac{F_0}{A_0} \quad \ldots\ldots\ldots\ldots 1$$

Therefore, the two areas (B) on both sides and the area between Zone G and Zone B are not important in Tensile Testing due to the first area (B) being the installation area with the two clamps in the tensile test machine, and it is therefore disregarded. The second one is also disregarded because it has a big area and the area is inversely proportional to the stress, which is therefore low and also disregarded. Therefore, the optimum area for measuring stresses is in Zone G due to it having the smallest area in the specimen.

And also the Engineering strain (ϵ_0) can be calculate from this test and it is defined by the relationship:

$$\epsilon_0 = \frac{(L_1 - L_0)}{L_0} \quad \ldots\ldots\ldots. 2$$

In fact, the stresses and strains calculated by the tensile test are not true. However, in any study, we need the true stress and strain because the simulation programs do not provide the needed real values. Furthermore, the true stress and strain are the real values.

The relationship between the engineering stress, strain and the true stress and strain are follows:

We assume that the volume remains constant:

$V_0 = V_1$ **SO**

$(A_0 \times L_0) = (A_1 \times L_1)$

$(\frac{A_0}{A_1}) = (\frac{L_1}{L_0})$

$\dfrac{A_0}{A_1} = \dfrac{\Delta L + L_0}{L_0} \quad \rightarrow \because \in = \dfrac{\Delta L}{L_0}$

$= \left(\dfrac{\Delta L}{L_0} + 1\right) \rightarrow = (\in_0 + 1)$

To find true stress equation:

$\sigma_t = \dfrac{F}{A_1}$

$\sigma_t = \dfrac{F}{A_1} \times \dfrac{A_0}{A_0}$

$\sigma_t = \left(\dfrac{F}{A_0} \times \dfrac{A_0}{A_1}\right) \qquad \rightarrow \qquad \sigma_t = \dfrac{F}{A_0} \times (1 + \in_0)$

$$\therefore \sigma_{t=} \sigma_0 \times (1 + \in_0) \ldots\ldots\ldots 3$$

To find true strain:

$\epsilon_t = \displaystyle\int \dfrac{dL}{L} \rightarrow = \ln(\dfrac{\Delta L}{L_0})$

$$\therefore \epsilon_t = \ln(1 + \in_0) \ldots\ldots\ldots 4$$

In this study, the tensile test was performed in the mechanical laboratory with a tensile test machine at room temperature. Standard test specimens were cut off by a laser cutting machine in three directions, the first of which was in the rolling direction (RD) or 0°, the second in a diagonal direction from the rolling direction (DD) or 45°, and the third in a transverse direction to the rolling direction (TD) or 90°. This was repeated for each of the four specimens but we only chose successfully specimens. The test was performed twice.

The first test was performed before heat treatment (mill annealing) (Fig. 22)
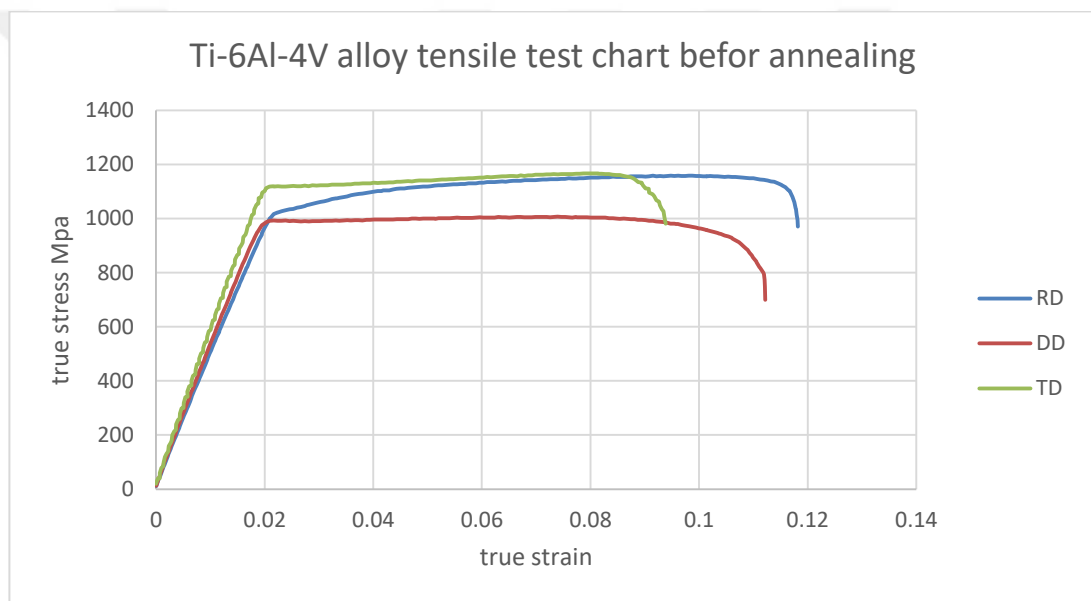
Figure 22: Tensile test results for Ti-6Al-4V alloy before annealing.

After completing the testing process and drawing the stress - strain curve, the yield stress (σ_Y) is calculated by 0.2 % offset from the point of origin .offset yield strength is reported as a stress (MPa) and is defined as the point where a line drawn parallel to the modulus line intersects the stress-strain curve see point B and line AB (Fig 23). Offset distance (AB) in (Fig 23) is the product of sample gage length and percent offset equal 0.2% (0.002) offset. All mechanical properties results calculated from the first tensile test are shown in the (Table 4) and (Table 5) appeared elongation percentage values. After applying the standard deviation rule to the results, the final results can be observed in the (Table 4).
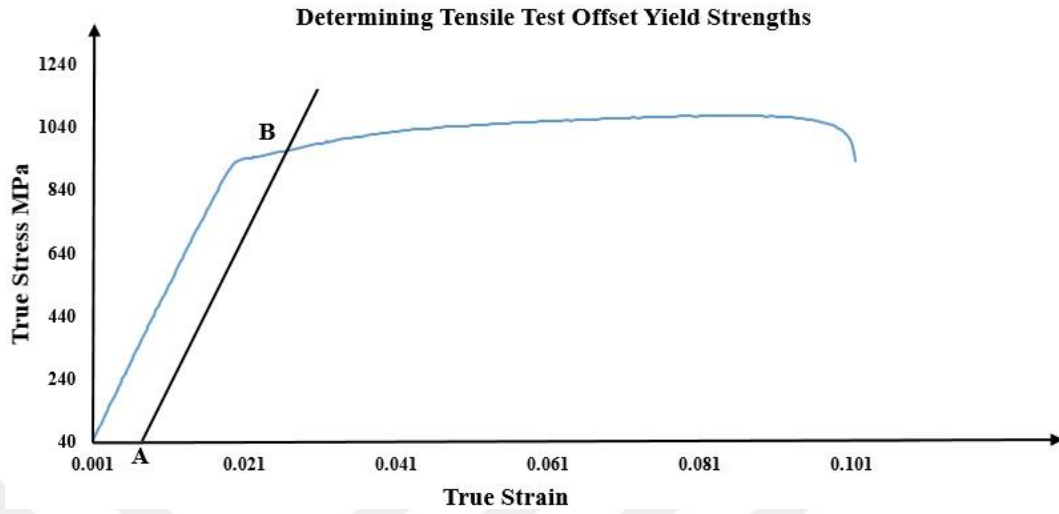
(a)

(b)
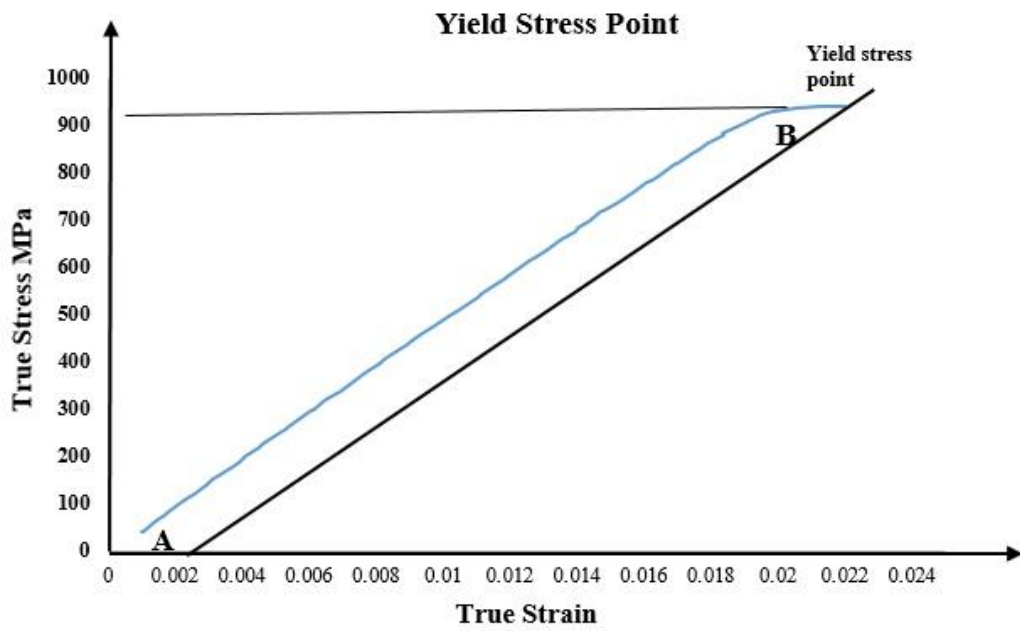
Figure 23: (a) Show mothed to determine yield stress from stress-strain curve by draw line (AB) from offset point with distance equal 0.002. (b) Mothed to determine yield stress from stress-strain curve (changing draw scale)

In fact these results cannot be accepted if compared with METALLIC MATERIALS AND ELEMENTS FOR AEROSPACE VEHICLE STRUCTURES (MMPDS) or (MIL-HDBK 5) standard. In this standard; the processes of heat treatments (mill annealing) on Titanium alloy (Ti-6Al-4V) sheet is necessary before any formation process, Therefore, heat treatment was performed on Titanium alloy (Ti-6Al-4V) sheets to obtain maximum ductility [33].

Table 4 : Tensile test results for (Ti-6Al-4V) alloy sheet before heat treatment

Tensile test values before Heat treatment for (Ti-6Al-4V) alloy						
Tensile test with (0°) Rolling Direction RD						
Parameters	**Specimen one**	**Specimen two**	**Specimen three**	**Average**	**Standard deviation**	**Final values**
Yield strength (σ_y) MPa	1018	1030	1024	1024	6	1024±6
Ultimate strength (σ_t) MPa	1143	1158	1149	1150	8	1150±8
Tensile test with (45°) Diagonal Direction DD						
Yield strength (σ_y) MPa	986	991	991	989	3	989±3
Ultimate strength (σ_t) MPa	996	1003	1007	1002	6	1002±6
Tensile test with (90°) Transverse Direction TD						
Yield strength (σ_y) MPa	1119	1102	1104	1109	9	1109±9
Ultimate strength (σ_t) MPa	1167	1148	1155	1157	10	1157±10

Table 5: Showing tensile test parameters before heat treatment.

Parameter	**Rolling direction RD (o°)**	**Diagonal direction DD (45°)**	**Transverse direction TD (90°)**
% Elongation	12	11	9

The second test was performed after heat treatment (mill annealing) (Fig. 24) for results and (Table 6) for the calculations of the mechanical properties and (Table7) appeared elongation percentage values. Results show great improvement, and these results are acceptable if compared with (MIL-HDBK 5) standard. The best case after heat treatment is the rolling direction, which is the closest case to the (MIL-HDBK 5) standard, so it has been adopted in the simulation process. The comparison between the tensile test results in the rolling direction and the (MIL-HDBK 5) appears in the (Table 8).
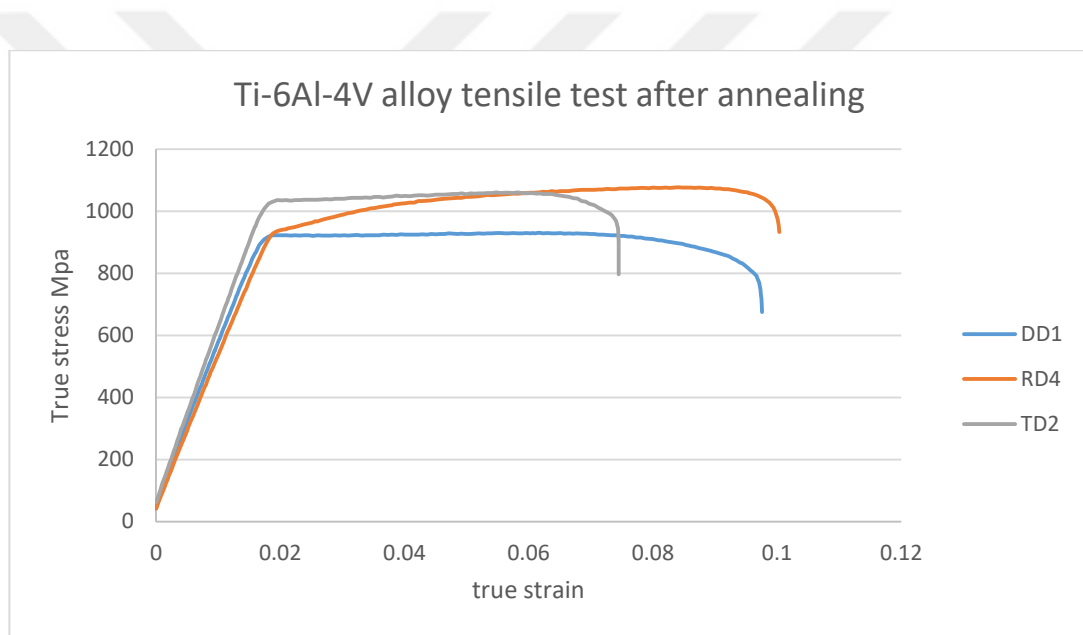
Figure 24: Tensile test results for Ti-6Al-4V alloy after annealing.

Table 6 : Tensile test results for (Ti-6Al-4V) alloy sheet after heat treatment

Tensile test values after Heat treatment for (Ti-6Al-4V) alloy						
Tensile test with (0°) Rolling Direction RD						
Parameters	Specimen one	Specimen two	Specimen three	Average	Standard deviation	Final values
Yield strength (σ_y) MPa	919	938	941	933	12	933±12
Ultimate strength ($\sigma_{t.}$) MPa	1041	1079	1076	1065	21	1065±21
Tensile test with (45°) Diagonal Direction DD						
Yield strength (σ_y) MPa	917	905	919	914	8	914±8
Ultimate strength ($\sigma_{t.}$) MPa	917	914	920	917	3	917±3
Tensile test with (90°) Transverse Direction TD						
Yield strength (σ_y) MPa	1025	1032	1028	1028	4	1028±4
Ultimate strength ($\sigma_{t.}$) MPa	1063	1060	1053	1058	5	1058±5

Table 7: Showing tensile test parameters after heat treatment.

parameters	Rolling direction RD (o°)	diagonal direction DD (45°)	Transverse direction TD (90°)
% Elongation	10	10	7

Table 8 : Comparing between the tensile test results in the rolling direction and the MIL-HDBK 5

parameters	Study results	MIL-HDBK 5 results
Yield strength (σ_y) MPa	933±12	924
Ultimate strength ($\sigma_{t.}$) MPa	1065±21	1014
Heat treatment temp.(°C)	705	704.4

3.3 Method and Principles of Hydro-Mechanical Deep Drawing

3.3.1 Introduction

As mentioned previously, hydro-mechanical deep drawing is a sheet metals forming process. It is a new technology using a pressurized fluid in a die cavity (chamber pressure), with a soft die being used instead of a hard die (female die) in conventional deep drawing to plastically deform. Hydro-mechanical deep drawing is a derivative from traditional deep drawing with a changed female die and filling with hydraulic fluids under pressure (Fig. 25).
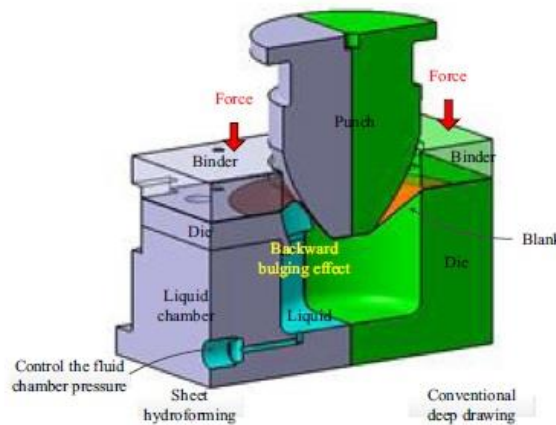
Figure 25: Showing compering between hydro-mechanical (gray) deep drawing and traditional deep.

When comparing hydro-mechanical deep drawing with traditional deep drawing, astounding features can be observed in hydro-mechanical deep drawing, such as low tool costs, higher dimensional accuracy, shorter cycle time, high drawing ratio, high surface finishing, complex shapes, etc. All these advantages have made forming sheet metal components with this method more competitive, not only for low-volume production but also, in some cases, for high-volume production, such as in the automotive manufacturing industry, where there is a need for low-volume production of body components.

3.3.2 Main Equipment for HDD System

3.3.2.1 Press

To form cups made from Ti-6Al-4V alloy sheets with the HDD process, a special hydraulic press machine has been used in this study (Fig. 26). The press parts move by means of hydraulic fluid pressure. High fluid pressure in the press machine is generated by a special high pressure fluid system (hydraulic unit). A special pipe system and control valves are required to transfer the compressed hydraulic fluid from the high pressure fluid system to the moving parts (Fig. 27). The two parts in the press machine require this pressure. The first is the punch movement which moves from down to up. The function of the punch is to form cups from sheets in hydro-mechanical deep drawing process. The second component is the blank holder which also moves from down to up. The function of the blank holder is to generate blank holder forces. These forces are necessary to fix the blank. Other parts in press machine are the fluid to be compressed, a female die to be filled with pressurized hydraulic fluid. This fluid is not for control but for formation as this pressure together with the punch is necessary to complete the forming process.

Figure 26: Showing hydraulic press system used in experimental work [28].
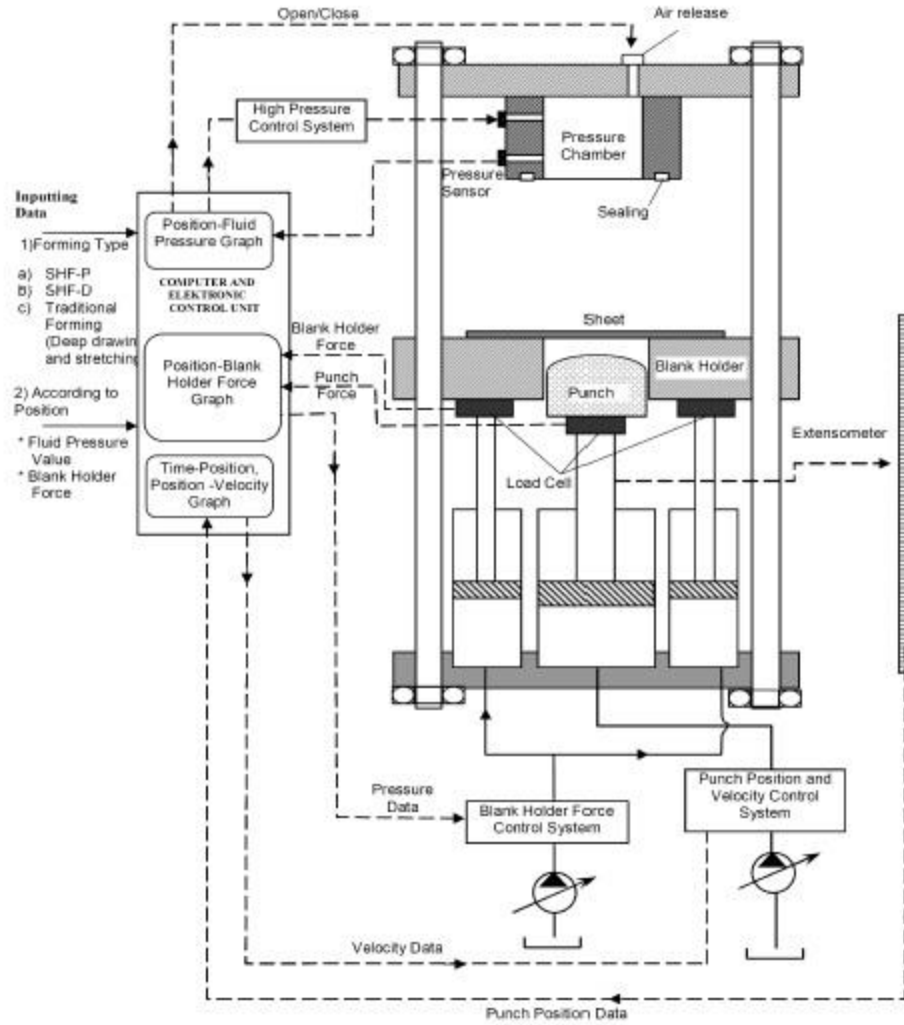
Figure 27: Hydraulic press parts with control system [28].

3.3.2.2 Tools

The hydro-mechanical deep drawing tools comprise two groups: the main tools and the assist system. The main tools consist of the punch, the die and the blank holder. The assist system consists of the hydraulic unit system, the control unit systems and other necessary parts (Fig. 27 and Fig. 28). The first part in this process is the punch, which is responsible for the final shape or final dimensions of the part. A precise radius of the punch is essential for this. This is due to the lack of a female hard die (a hard die is used

in the traditional deep drawing process). It is replaced by a soft female die with a cavity (with a pressurized fluid) in the hydro-mechanical deep drawing process.
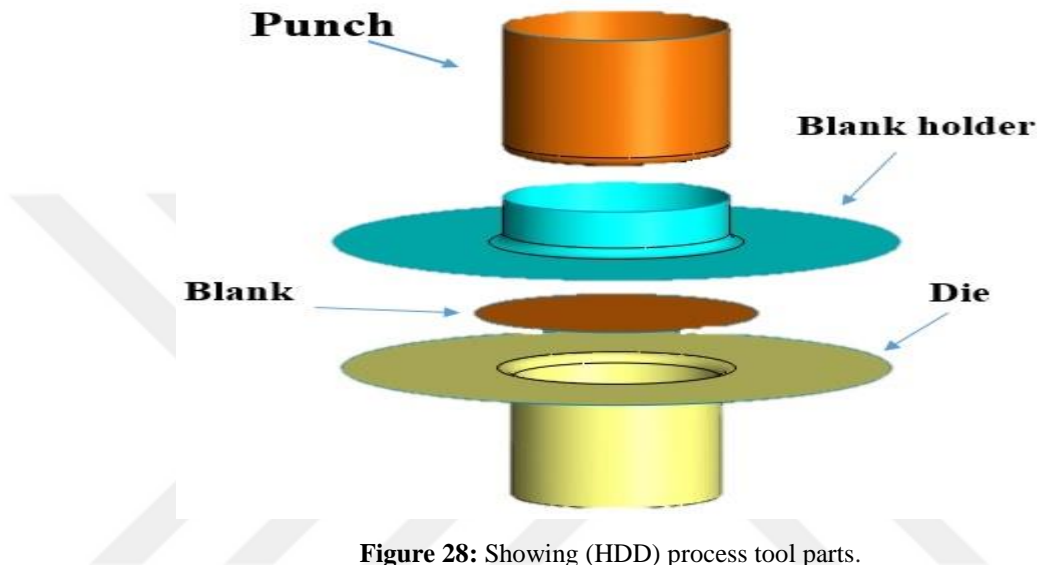
Figure 28: Showing (HDD) process tool parts.

The second part in the forming tools is the female die with cavity filling by pressurized fluid. The pressurized fluid in the cavity is responsible for two important situations in the mechanism of the forming parts. The first is pre-bulge pressure and the second is the main forming pressure (chamber pressure). The blank holder is the third part of the forming tools. Its function is to fix the blank over the female die (drawing ring). The pressures or the blank holder force (BHF) generated from the blank holder and pressurized fluid in the cavity are very necessary for forming parts and reducing any defects. The female die is connected to a hydraulic unit to compress fluid into the cavity at high pressure. The cavity has a safety valve connected to it to reduce any excess pressure during forming.

3.3.3 Principles of Work in the Hydro-Mechanical Deep Drawing Process

In this process, the female die set in a hydro-mechanical deep drawing process consists of a drawing area by pressure cavity. The pressure cavity is filled with a hydraulic fluid. The blank is deformed by the mechanical pressing action of the punch into the pressure cavity. The punch penetration into the hydraulic medium generates a pressure increase due to fluid compression that is controlled using a pressure control valve. The blank being drawn is pressed firmly onto the punch due to pressure build-up. This increases the friction between the punch and blank and hence higher forces as compared to that in conventional deep drawing, which can be transferred to the deformation zone (Fig. 29). The metal undergoing hydro-mechanical deep drawing thus fractures at a much higher stress value than in the conventional deep drawing. Some process parameters can affect the success of the process, including cavity pressure, blank holder force, tool profile radii, punch speed, friction between blank and tool components and the pre-bulge pressure.
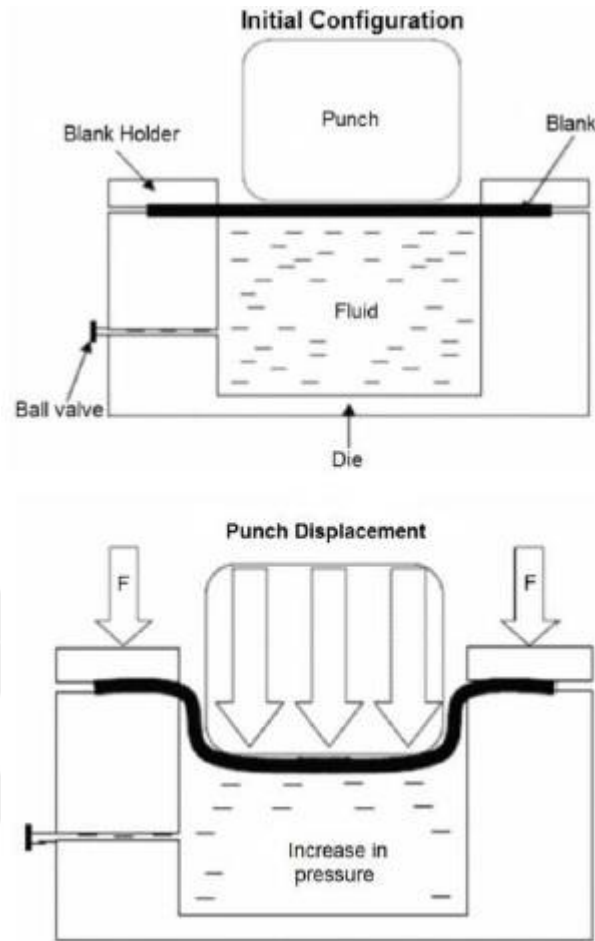
Figure 29: Showing cup forming by using hydro-mechanical deep drawing [29].

3.3.4 Main Forces in the Deformation Area

In the traditional hydro-mechanical deep drawing process, the friction forces are the most important forces to form parts. Friction forces are generated as an effect of the punch movement toward the blank and coming into contact with it. The blank holder movement and blank create another friction force. Other forces are generated by the pressurized fluid in the cavity. These forces start before the punch movement starts. The pressurized fluid affects the lower surface of the blank leading to a bulge in the blank. The process starts while the punch moves forward toward the blank. The blank is, of course, fixed before that by blank holder. The punch force, blank holder force and hydraulic fluid pressure can be calculated with mathematical equations.
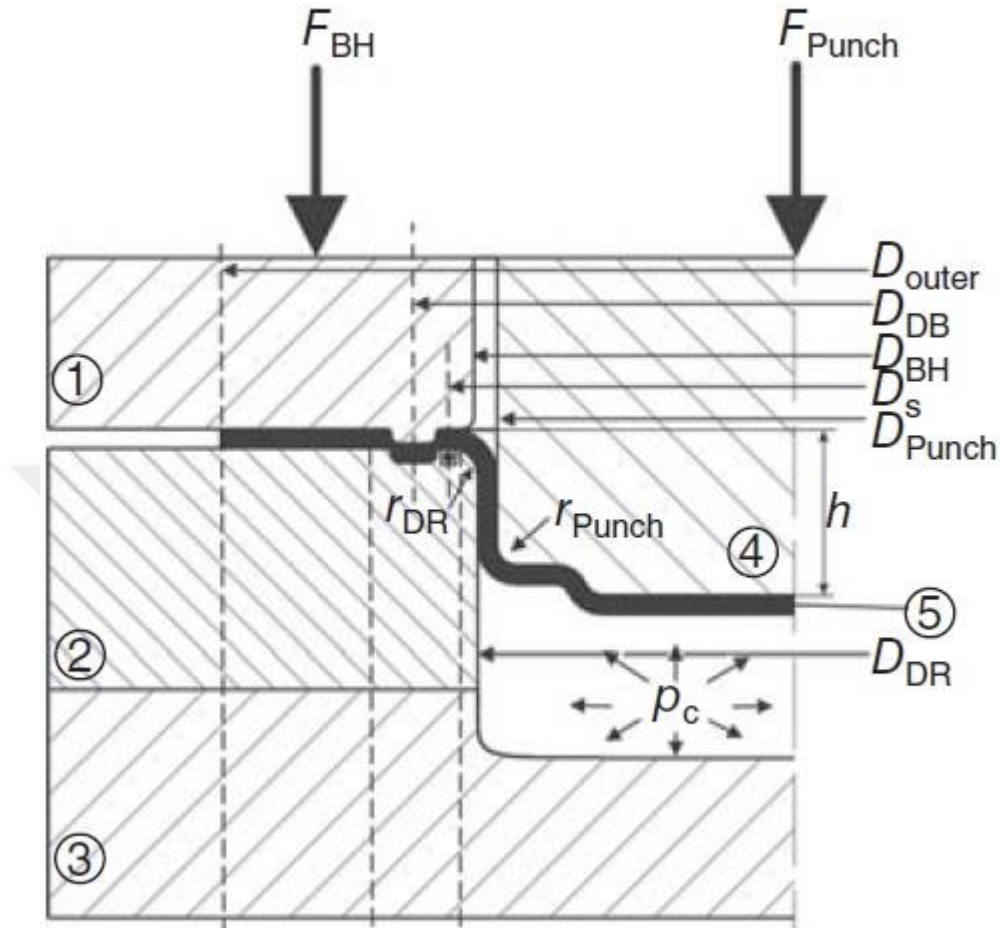
Figure 30: Showing a deformation area with main dimensions, forces and parts (1) blank holder (2) drawing ring (3) die (4) punch (5) blank [21].

To calculate the punch force, we should know the friction forces in the deformation area. After the punch moves toward the blank and comes into contact with the blank, many are forces generated in this area (Fig. 30). The friction force between the blank holder and the blank ($F_{friction\ BH.B}$) is generated against the blank forming flow, as is the friction force in the drawing ring.

The upper female die and the blank ($F_{frection\ DR.B}$) work against the blank forming flow. In addition, one has to consider the bending force (F_B) to bend the sheet around the radial of the draw ring edge as well as the draw bead force (F_{DB}) which is built up by bending and friction forces acting on the blank as a restraining force when pulling the blank through the draw bead. The ideal force (F_{id}) is the punch force for the ideal condition where there are no friction or bending forces. This force cannot be calculated in

reality. It is found in the area between the outer diameter of the blank $(D_{B.out})$ and the diameter of the punch (D_P), and it can be calculated with the following equation:

$$F_{id} = D_P \, \pi \, t \, \sigma_{mf} \, \ln \frac{D_{B.out}}{D_P}$$

Where a medium flow stress (σ_{mf}) define as:

$$\sigma_{mf} = 0.5 \, (\sigma_{Bfo} + \sigma_{BfDi})$$

Before the punch moves, the lower surface of the blank is pressed by the chamber pressure (bulge pressure), against the direction of the punch. After the punch moves and comes in contact with the other side of the blank, the vertical force acting on the punch in this area becomes:

$$F_{P.counter \, pressure} = \frac{\pi}{4} \, P_c \, D^2_{contact}$$

The next step after the punch comes into contact with the blank, the punch movement continues and other forces appear. We know that the blank is bulging upwards due to the counter pressure opposing the direction of the punch movement. At this moment, a critical gap is seen between D_{BH} and $D_{contact}$ (Fig. 30) with respect to the yield stress (σ_y) and the thickness (t) of the blank. The force $F_{bulde.vertical}$ is acting on the contact point on the bulge:

$$F_{bulge.vertical} = \frac{\pi}{4} \, P_c \, (D^2_{BH} - D^2_{contact})$$

The stress in the same area can found thus:

$$\sigma = \frac{P_c}{4t}(D_{BH} - D_{contact})$$

In the same area, other forces are generated from the bulge acting on the punch. This force is defined by the equation:

$$F_{punch.bulge} = \sigma D_{contact}\pi t$$

Moreover, in the same area, a force is generated from bulge acting on the blank holder. This force can be found thus:

$$F_{BH.bulge} = \sigma D_{BH}\pi t$$

The force generated between the blank and the drawing ring, particularly in the gap between them, the resulting vertical force acting on the blank can be calculated thus:

$$F_{BH.counter\ pre.} = \frac{\pi}{4}P_C\ (D_S^2 - D_{BH}^2)$$

All these forces resulting from the formation of parts by punch movement forward toward the blank and punch can found by the following equation:

$$F_{punch} = F_{id} + F_{frection\ BH.B} + F_{frection\ DR.B} + F_{punch.bulge} + F_{BH.counter\ pressure} + F_{DB}$$

Other important force effects in this process include the blank holder force, which plays an important role in the success or failure of hydro-mechanical deep

drawing processes. Low blank holder force may result in the appearance of wrinkling in the flange area of a product. For high blank holder force, a premature rupture is likely to occur. Blank holder pressure (P_{HB}), which is a normal pressure between the blank and blank holder and between the blank and the draw ring, should be set suitably to avoid wrinkling in the area between the blank holder and draw ring. For axi-symmetric parts, it can be written as follows:

$$P_{HB} = 0.002 \dots \dots 0.0025 \left[(\beta_\circ - 1)^3 + 0.5 \frac{D_{punch}}{100t_\circ} \right] \sigma_{UTS}$$

3.3.5 Cavity Pressure Curve

A cavity pressure curve includes three different factors, namely initial pressure, pressure path and the final pressure reached at the end of the process. Exploiting the properties of the pressure curve, a rather simplified method based on FEM can be utilized instead of the upper bound technique. Since the punch penetration volume during the forming is also monotonically increasing, similarly to the pressure curve the pressure path is assumed to be proportional to the punch penetration volume [22].

CHAPTER FOUR

SIMULATION AND EXPERIMENTAL STUDY

4.1 Introduction

Finite element analysis is important to many industries, especially those that need to predict failure of a structure, object, or material when under unknown stresses as it allows designers to determine all of the theoretical stresses within a structure. Finite element analysis uses a complex system of points (nodes) that comprise a grid called a (mesh). The mesh is programmed to contain all the material, properties, and other factors that constitute the structure and determine how it will respond to certain load conditions, such as thermal, gravitational, pressure or point loads. The nodes are then assigned a density throughout the material, all depending on the stress levels anticipated in a certain area.

In this study, finite element analysis (simulation) has been used to understand Ti-6Al-4V alloy and stainless steel (304) sheets behavior while forming cups. Cups are formed by applying the hydro-mechanical deep drawing process. To do so, many steps are followed. In the first step, the SOLIDWORKS program was used to draw geometric tools, after which the DYNAFORM program was used to add parameters and create a mesh for every part. In the final step, the LS-DYNA program was used to analyze the parameters and select the best conditions to form a cup.

In the experimental part, optimal parameters were taken from the numerical study. These selected parameters cannot used directly, so they are re-calculated to be ready for the experimental work. The experimental work was performed twice with two different simulations and tool geometries. In Chapter Five, the results are compared and discussed.

4.2 Finite Element Simulation Work

4.2.1 Simulation Theory

The finite element method (FEM) is a numerical technique by which differential equations are solved nearly up to a selected degree of accuracy .In FEM, the manner of a continuum, which is normally impossible to define exactly, is approximated by idealization. For this purpose, the shape and behavior of the continuum is redefined by a mesh which is collected of finite collection of sub-domains called finite elements and nodal points where the values of the function (displacements) and its derivatives (velocity and acceleration) are specified.

Also, the relationship between the unknown displacement and known forces at the nodes are determined with a formulation, which can be either linear as in Eq. 1, where the structural stiffness is independent of displacement, or a non-linear formulation as in Eq. (2), where the structural stiffness is dependent on displacement.

$$\{F\}= [k] \cdot \{u\} \ \text{.......................} \ (1)$$

$$\{F\}= [k \ \{u\}] \cdot \{u\} \text{....................} (2)$$

The sources of nonlinearity in the finite element analysis can be classified as material nonlinearity, contact nonlinearity and geometric nonlinearity. Metal forming simulations are non-linear problems and they should be answered by using non-linear formulation.

The number and density of mesh depends on the requirements of the process to be simulated. The element size in the mesh should be small enough to represent all the details in the geometry and large enough to avoid unnecessary time consuming calculations in order to be cost efficient. For non-deformable tools, mesh is only representation of the geometry, whereas for deformable bodies, the finite elements are the representation of material with a simplified behavior in small pieces. Various material behavior models are

44

used in FEM. Rigid-plastic and elasto-plastic are the most commonly used material models in metal forming simulation. The former does not require the consideration of the linear kinematics of the finite deformation; hence, the formulation is less time consuming, more reliable, and robust. On the other hand, elasto-plastic material model should be used for residual stress analysis and net shape forming process simulations in which the elastic strains cannot be neglected. In elasto-plastic material model, the elastic behavior is taken to be linear and the plastic response is usually modeled using the Levy-Mises yield criterion. According to the requirements, element type used may also show variety in the finite element simulations. In bulk metal forming, only continuum elements are used, whereas in sheet metal forming, surface elements are preferable due to the high surface to volume ratio of the workpiece. There are four different types of elements available for the analysis of sheet metal forming processes. In sheet metal forming processes for which bending occurs over a bending radius larger than roughly ten times the sheet thickness , membrane elements can be used, However for the deep drawing simulations, shell elements are more applicable and they are divided in to two groups which are thin and thick shell elements. Continuum elements are rarely used in sheet metal simulations, but sometimes for hydroforming and blanking simulations, they are appropriate to use. No matter surface elements or continuum elements are used, the use of triangle or tetrahedral elements in the deformable mesh should be prevented where possible. Providing the robustness and due to contact problems, it is advisable to use low order element having four nodes and using linear shape functions. In addition, two different time integration schemes, namely implicit and explicit algorithms are used in FEM. Implicit algorithm enables a full static solution with convergence control whereas explicit algorithm is more robust and there is no check [32].

4.2.2 Tools Drawing

All the necessary tools (punch, blank holder, die and blank) to form cups in the hydro-mechanical deep drawing process were drawn by the SOLIDWORKS program as surface entities (Fig. 31). Only one quarter of the geometry was modeled due to axisymmetric geometry. The tools were drawn with geometry dimensions (Table 6). Everything was saved as an IGS file for later use. This file was then imported by the Dyanform program for insertion of all simulation parameters.

Table 9: Tools geometry dimensions.

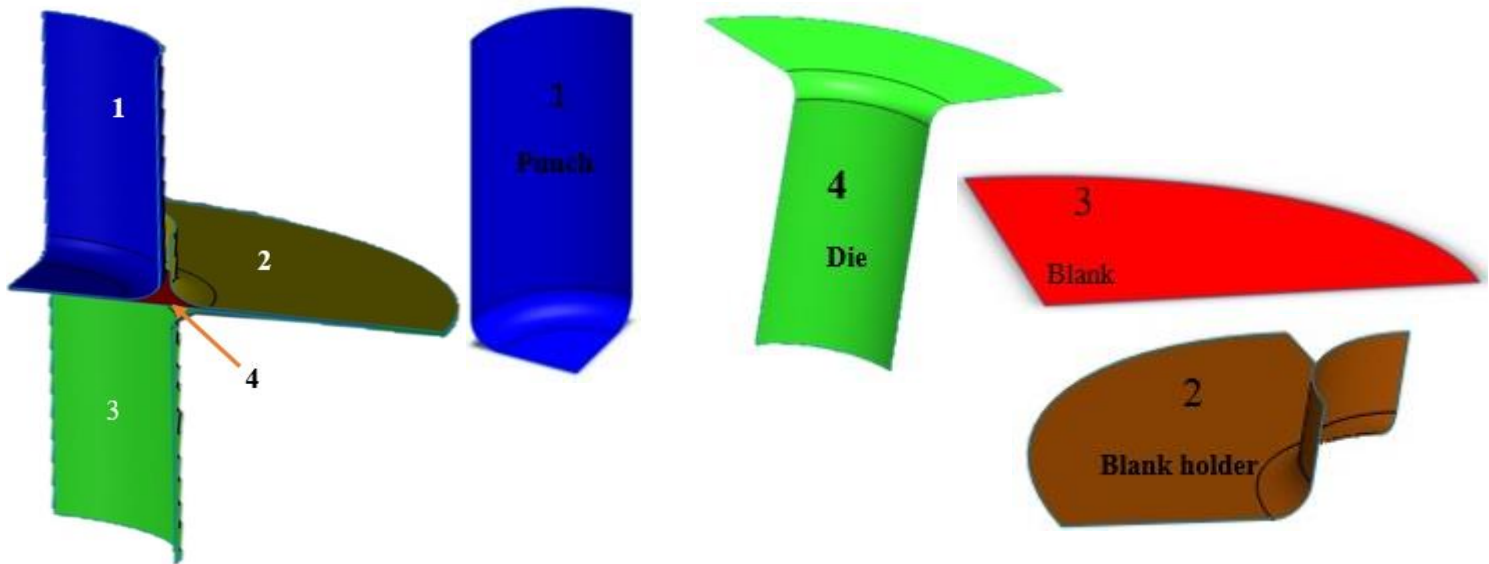| No.	Describe	Symbol	Measurement(mm)
1	Punch diameter	D_P	40
2	Punch nose radius	r_p	5-8
3	Die diameter	D_D	43
4	Die radius	r_D	5-8
5	Clearance between punch diameter and die diameter	c	3 (1.5 in each side)

Figure 31: HDD tool geometry drawing by (SOLIDWORKS) program assembly.

4.2.3 Modeling of Matel Alloy

Another important part of the simulation using the finite element model (FEM) is the selection of an appropriate alloy model. The DYNAFORM program was used for this purpose. The required properties of the blank Ti-6Al-4V alloy sheet were obtained from a tensile test after heat treatment (annealing process). The material is assumed to be piecewise, linear or plastic. Material properties such as mass density, Young's modulus of elasticity, ultimate stress and Poisson's ratio are given as inputs to perform finite element (FE) calculations. The true strain-stress curve was also used as a result of the tensile test (see Fig. 32 and Table 7).
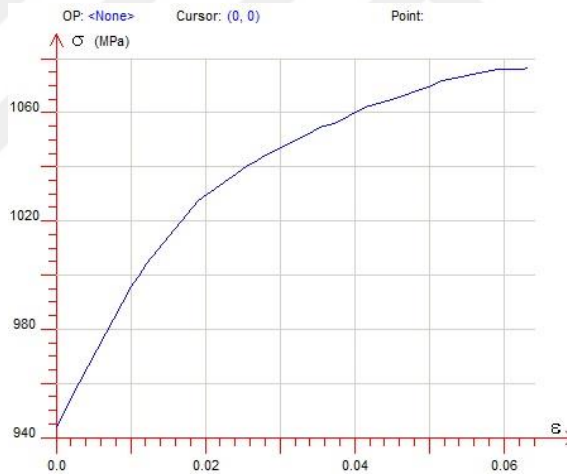

Figure 32: Show true strain – stress curve used in material modeling.

Table 10: Physical properties using in simulation.

Alloy name	Miss density	Young's modulu's	Poisson's ratio
Ti-6Al-4V	4.43 e-009	113800.0	0.342

4.2.4 Modeling of Tool

In the DYNAFORM program in the performance of the simulation, the tool variables, such as coefficient of friction, punch travel direction, mesh measurement, tool geometry definitions and work time, are very important. The tools mesh measurement are defined such that all parts must equal 4 except for the blank, which equals 1.5 (Fig. 33). The punch movement is defined in the negative z-direction, which corresponds to the direction of the punch axis. Additionally, a blank holding force (BHF) is applied onto the blank by the blank holder in the negative z-direction. As for the die, its location is on the positive z-axis. Because of the effect of the chamber pressure, the coefficient of friction between the die and blank equals 0.05, and between the blank holder and blank, it also equals 0.05. However, the coefficient of friction between the punch and blank equals 0.25. Note that the coefficient of friction between the punch and blank is higher than the other coefficients because it is one of the main forming forces.
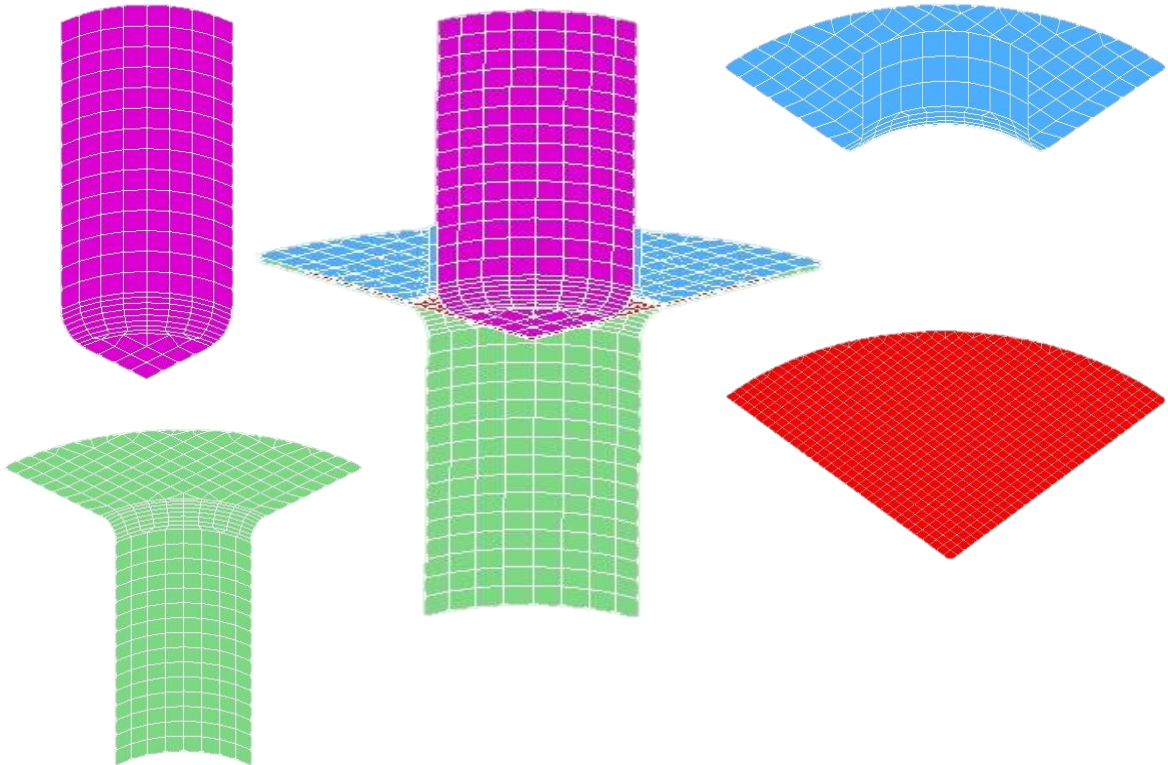

Figure 33: Showing tools mash.

4.2.5 Modeling of Process Parameters and Boundary Condition

In the case of hydro-mechanical deep drawing (HDD), the chamber pressure has to be applied on the surface of the blank. The chamber pressure specifies all nodes at the loading ring on the blank in the opposite direction of punch travel by applying the pressure boundary conditions.

There is also provision for applying the chamber pressure by the element normal. In this case, it is necessary to ensure that the normal are oriented downward because the pressure always acts against the element normal [30]. Before the forming starts by punch movement in the HDD process, the blank is fixed by the blank holder over the drawing ring. The blank holder force is defined in the DYNAFORM program as the relationship between time and force. After forming has started, the punch displacement is defined as the relationship between displacement and time. This curve is used to define the motion of the punch to a depth that is allowable for a particular draw ratio. The blank holding force (BHF) is applied on the blank by the blank holder in the negative z-direction. The optimum blank holding pressure increases with an increase in the peak chamber pressure. The required blank holding force is calculated using the optimum blank holding pressure and the flange area onto which the BHF is applied. This method roughly gives the blank holding force and to arrive at the optimum values, the BHF is varied within a certain range at every stage. The process parameters, BHF and peak chamber pressure are varied in a range and the optimum values of these are identified at every stage that will produce a better thickness (i.e., minimum thinning) in the simulation. The pressure chamber path (variation of pressure vs. time) that is used to simulate the process is an important variable. The pressure chamber path starts before the punch movement to bulge the blank (pre-bulge pressure), and chamber continuously increases the pressure until the end of the process. This is important for the thickness distribution in the cup wall.

4.2.6 Simulation Sequence

In order to understand everything clearly, the simulation is accomplished by sequential steps. The first step is to draw the tools using the SOLIDWORKS program and saving them as (igs) files. The second step is to import these files into the DYNAFORM program as well as import the required parameters that were installed and saved as .dyn files. The final step is to analyze the information and study it with the LS-DYNA and Eta Post Processor programs.

4.3 Experimental Work

To do the experimental work, tools and machine are used. A punch, die, and blank holder are used as tools in this process. A special press with double action movements is used as the machine in this process (Fig. 25). All the tools are fixed with the press (Fig. 36).

4.3.1 Forming Tools

Hydro-mechanical deep drawing tools consist of a punch, blank holder and die (Fig. 34). The punch radius (Fig. 35) is responsible for the final shape of the parts. In this experiment, the punch moves from down to up (Fig. 36). The second part is the blank holder the function of which is to fix the blank over the die during forming i.e., it generates the blank holder force (BHF). The blank holder moves down to up (Fig. 36). The third part is the die the function of which is to form cups by keeping fluid in the cavity under pressure. The die is connected with a filling pipe and a relief valve (Fig. 37).
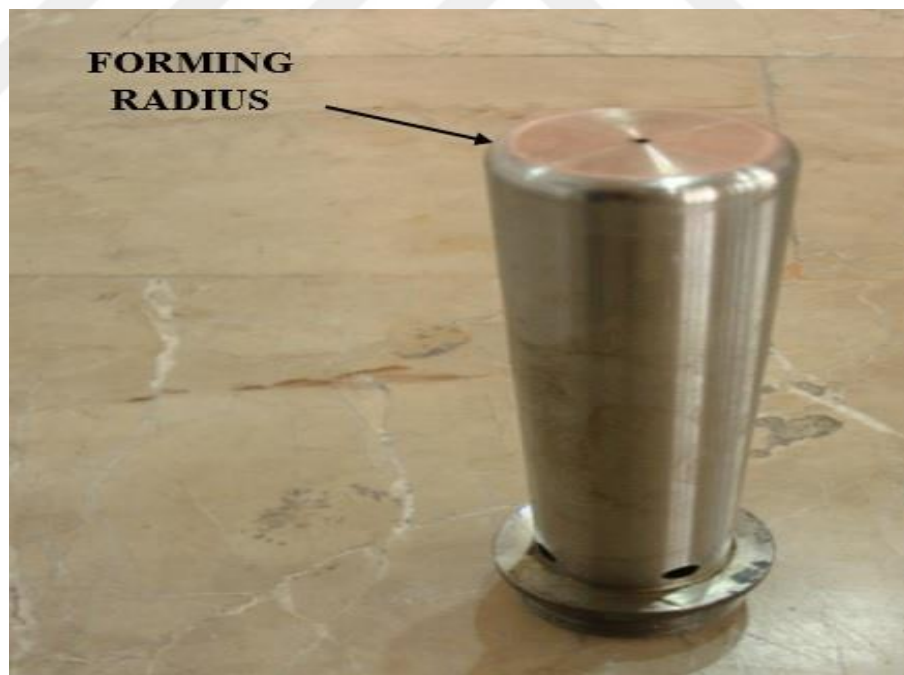
Figure 34: HDD tools parts.

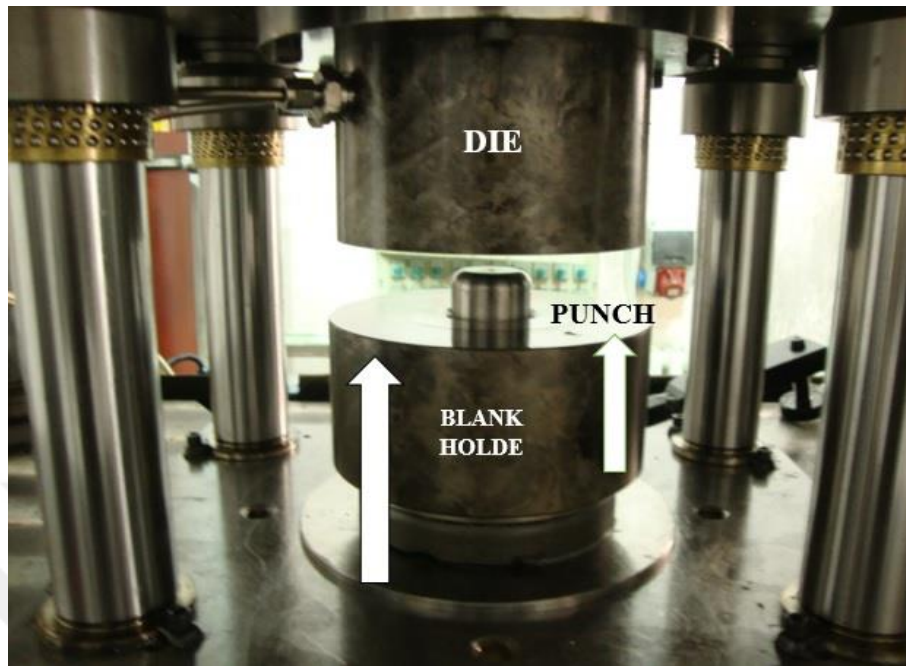**Figure 35:** Radius forming in punch.

Figure 36: HDD parts assembly with press and directions.

4.3.2 Press Control and Work

As mentioned earlier, the hydraulic fluid is responsible for the motions of all press parts. In this press, two parts have motions: the punch and the blank holder. Press control is carried out by the control panel (Fig. 37). This panel (PLC) controls and reads some parameters. After holding the blank between the blank holder and the die, the press control changes to auto through the use of a changeover select switch (Fig. 37). By using the WIN-PED program, all parameters during forming appear on the PC screen and it registers all variables as curves. To start the experimental work, every tool should be installed with the press (Fig. 38), as well as connecting the die with the filling pipe and relief valve (Fig. 39).
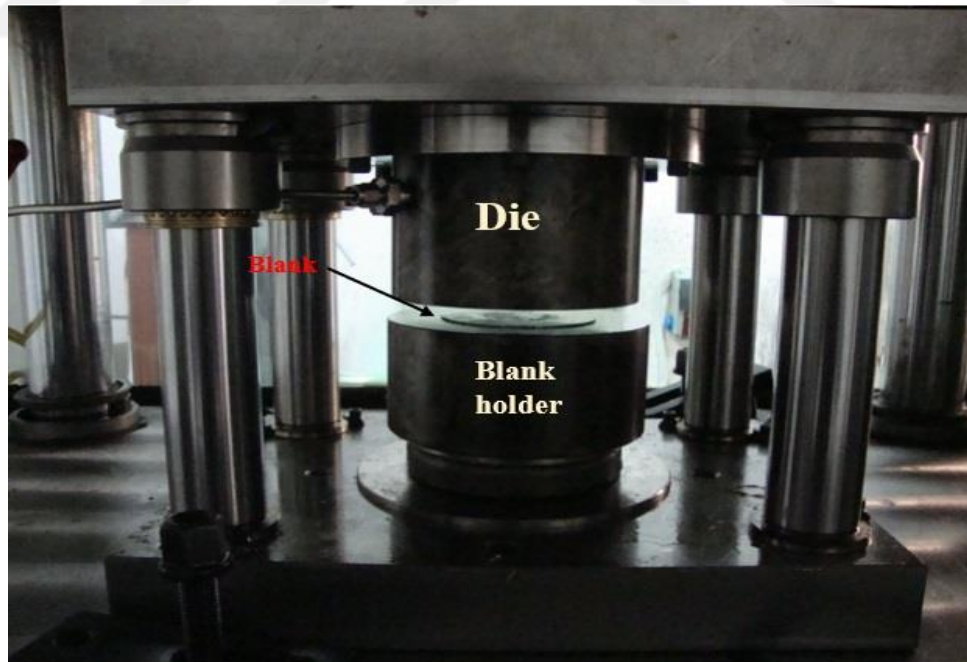
Figure 37: Control panel.

Figure 38: Blank position before forming.

Figure 39: Filling valve and relief valve connected with die.

After finishing all these necessary preparations, all parameters which were calculated via the simulation are installed on the PC. These parameters cannot be used directly because we should apply some mathematical equations to make them principle to the experiment conditions. After finishing the calculated parameters, a blank is prepared in many steps, the first of which is heat treatment (mill annealing) (Fig. 40). The second step is the use of wax and nylon; the two sides of the blank are painted with wax and nylon except for the area being punched forward due to the decreased friction force between the blank holder and the blank. The same application of wax and nylon occurs on the other side between the die and blank (Fig. 41).
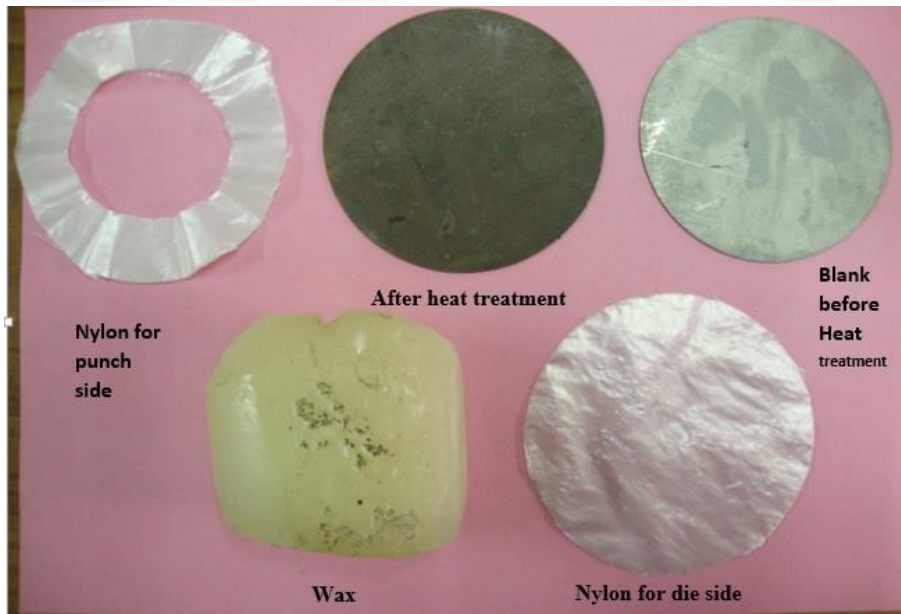
Figure 40: Blanks after finished heat treatment.

Figure 41: Nylon and wax used to paint and cover blanks.

CHAPTER FIVE

RESULTS AND DISCUSSION

5.1 Introduction

In this chapter, the results of the simulation and the results of the practical experiments are discussed. This chapter is divided into two sections pertaining to Experiment 1, and Experimental 2. In the first section, all results and data are presented from the numerical and experimental study processes. Similarly, in the second section, all results and data are presented from the numerical and experimental study processes. We then review, discuss and compared all experimental results.

## 5.2 Numerical Results for First Study

The objective of the numerical study was to determine the appropriate conditions to form a Ti-6Al-4V alloy sheet. This study did so by forming a radius $r_p = 5$ mm. After completing the analysis, the results were studied and classified as follows:

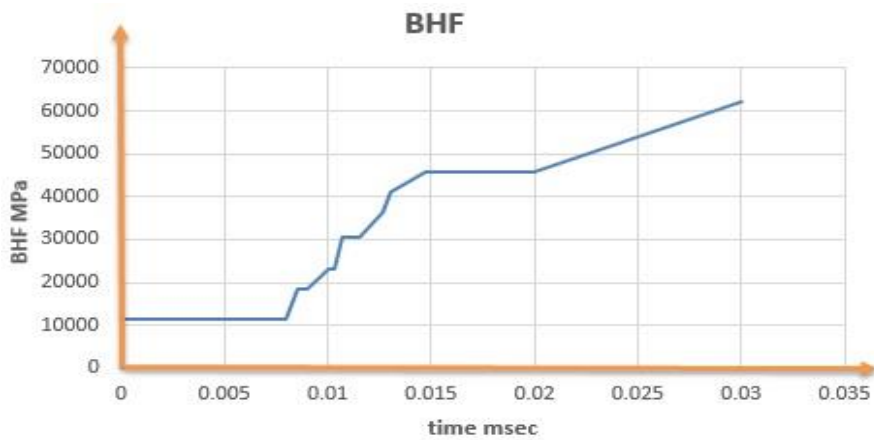### 5.2.1 Finite Element Simulations with Increased Blank Diameter

Simulations were carried out by increasing the initial blank diameter. The drawing ratio percentage and cup wall thinning were also studied. All necessary parameters (punch displacement, pressure path, and blank holder force) were used (Fig. 42), and every curve was plotted with respect to time.

(a)
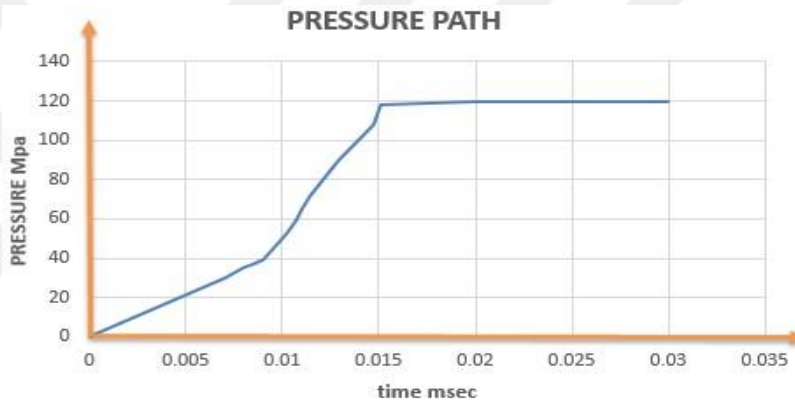
(b)

(c)

Figure 42: Showing finite element simulation of HDD process parameters **(a)** punch displacement curve **(b)** pressure path curve **(c)** blank holder curve.

In this case, four attempts were made, and in all cases over 95 mm, all attempts were failures; therefore, 80 mm, 85 mm, 90 mm and 95 mm were selected. The simulation was started with an 80 mm diameter. Good results were calculated and the maximum wall thinning percentage value was 9.862% (Fig. 43). The second simulation used 85 mm, also with good results and maximum wall thinning percentage value of 11.144% (Fig. 44). The third successful simulation occurred with 90 mm and a maximum wall thinning percentage value of 13.918% (Fig. 46). The final simulation was performed with the 95 mm diameter, yielding a maximum wall thinning percentage value of 19.195% (Fig. 45). Simulation results for the Ti-6Al-4V alloy sheet in the HHD process showed that the maximum diameter can be equal to 95 mm, which means the largest draw ratio being reached is (2.4). Table 8 shows the simulation details.
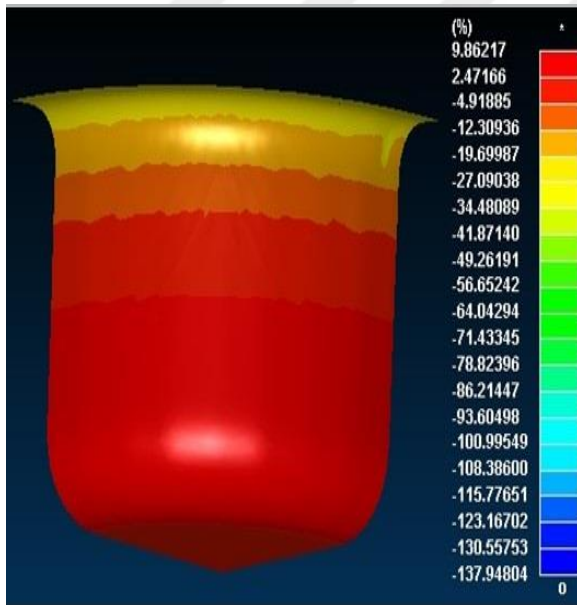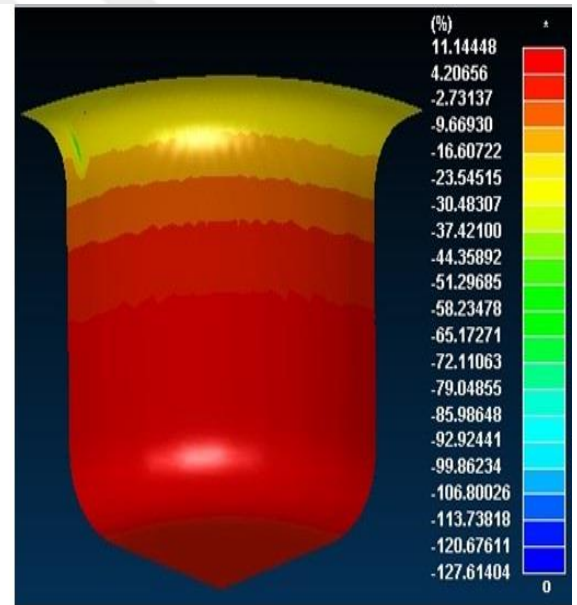

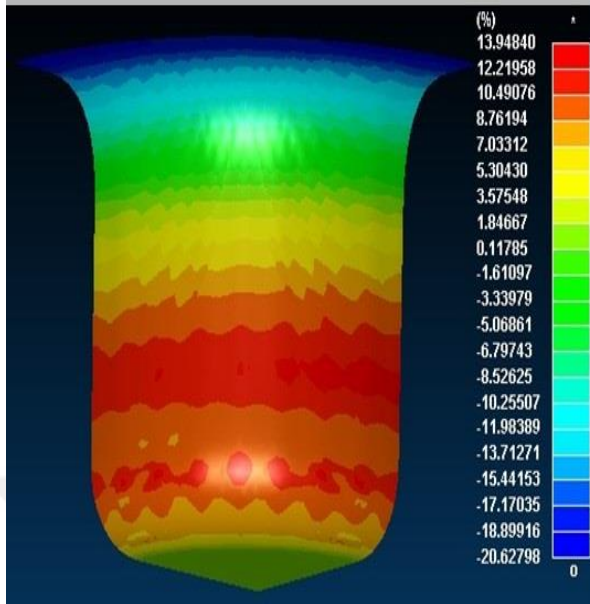**Figure 44:** FEM of dia. =80 mm

Figure 43: FEM of dia. = 85 mm
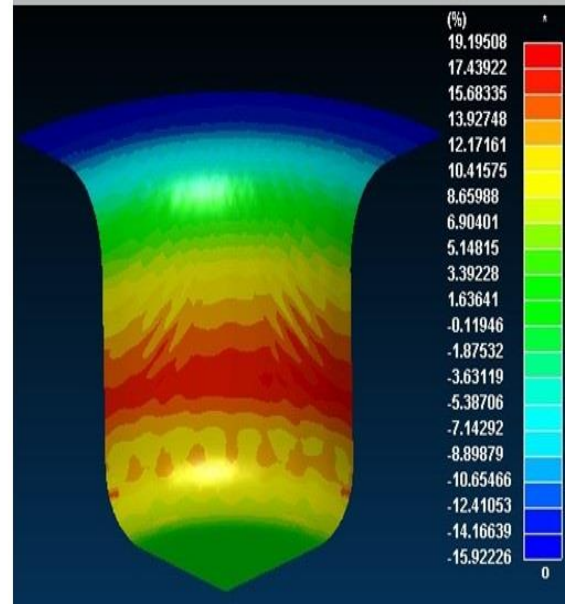
Figure 46: FEM of dia. = 90 mm.   **Figure 45:** FEM of dia. = 95 mm

Table 11: Showing max. Drawing ratio of (Ti-6Al-4V) alloy sheet.

No.	Diameter mm	Thinning %	Drawing ratio	Situation
1	80	9.862	2	Successes
2	85	11.144	2.125	Successes
3	90	13.918	2.25	Successes
4	95	19.195	2.375≈ 2.4	Successes
5	Over 95			Failure

5.2.2 Finite Element Simulation with Changing Blank Holder Force

In this item, the optimal blank holder force is calculated. After the maximum blank diameter is found, the cup wall thinning percentage will decrease via the enhanced blank holder force with this diameter. This was found by increasing and decreasing the blank holder force. After taking the fourth attempt in Table 8 as a reference, four more attempts were made. Two attempts were made with blank holder force values 10% and 20% above the reference blank holder force values. The first attempt appeared as a bad result with cup wall thinning increasing from 19.195 % to 20.053% (Fig. 47), which means that the attempt was a failure with regard to the thinning parameter. It was not necessary to make

further attempts above this value as we know the percentage of increase in cup wall thinning. There was a 20% increase above the reference blank holder force and the results show an increase in cup wall thinning from 19.195 % to 22.07%, which was also a failed attempt (Fig. 48).
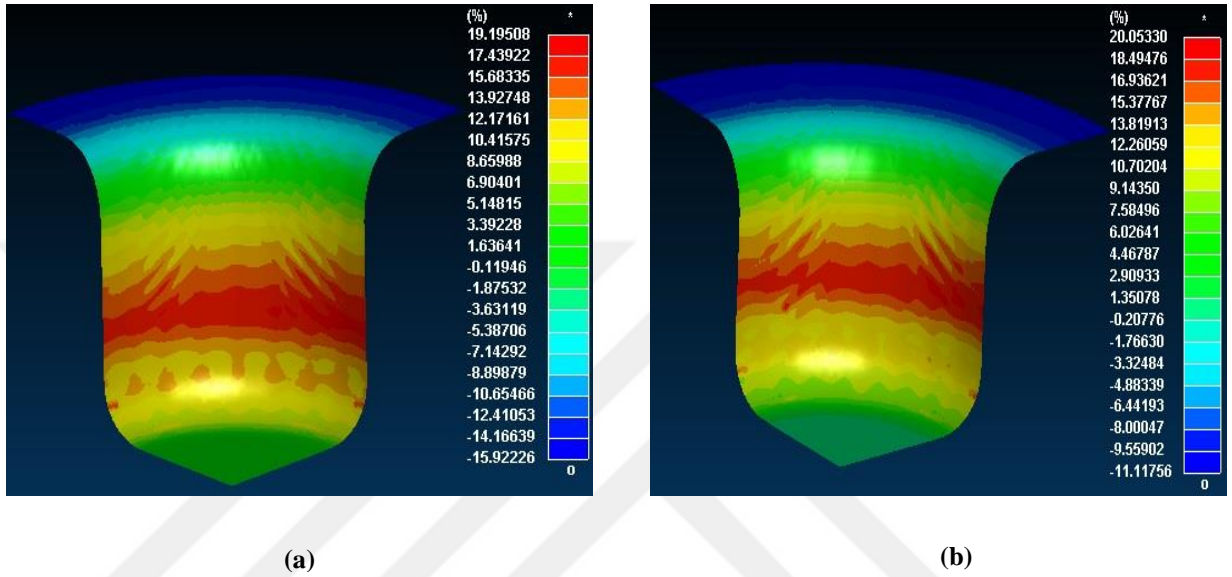
Figure 47: Showing cup wall thinning effective by changing blank holder force **(a)** reference **(b)** increasing blank holder force (10%) from reference force.

Figure 48: Showing cup wall thinning effective by changing blank holder force **(a)** reference **(b)** increasing blank holder force (20%) from reference force.
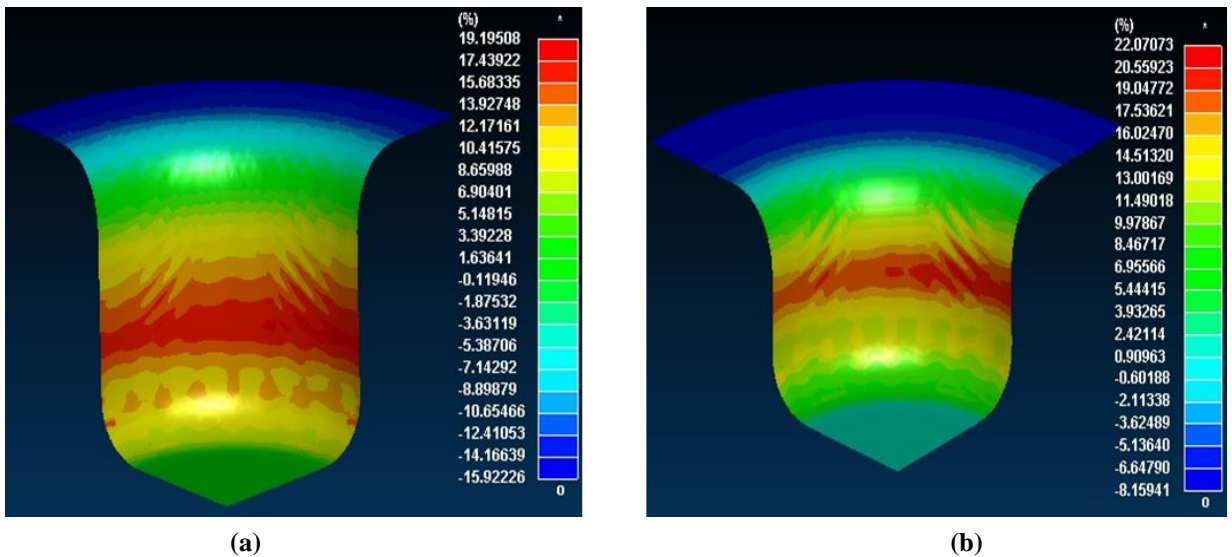
This means we should go to the opposite side to reduce cup wall thinning. A blank holder force that is 10% lower than the reference blank holder force is taken. The results indicate an improvement in the thinning parameter from 19.195 % to 18.081% (Fig. 49). These results encouraged us to reduce the blank holder force beyond 10% to produce better results. There was a 20% reduction in the blank holder force, and the results fell from 19.195 % to 16.807 % (Fig. 50). After this attempt, the simulation did not succeed. (Fig. 51) shows all readings of the thinning percentage.
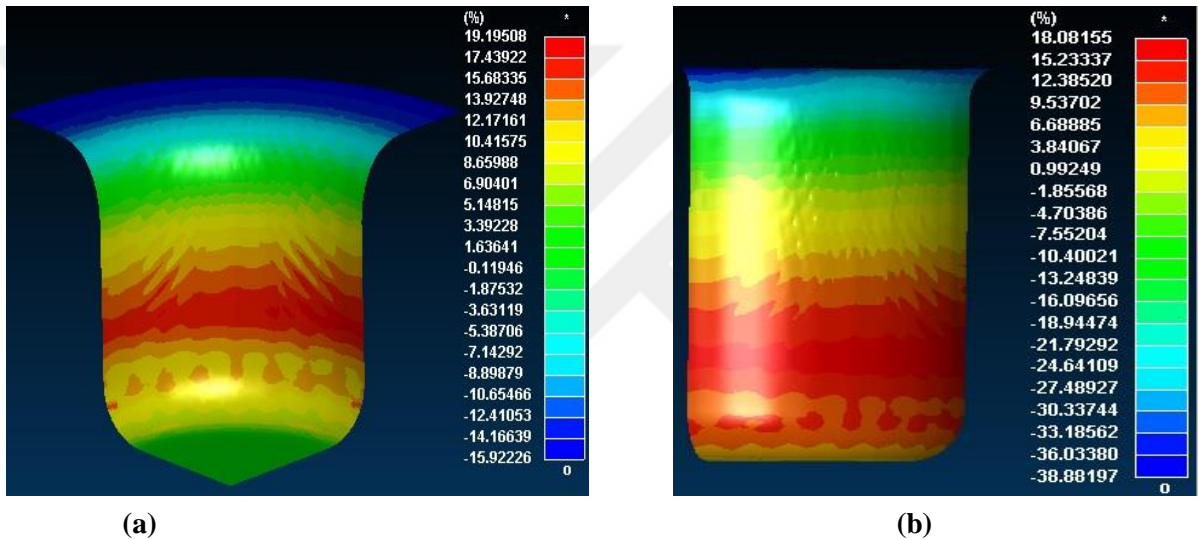

(a)   (b)

Figure 49: Showing cup wall thinning effective by changing blank holder force **(a)** reference **(b)** decreasing blank holder force (10%) from reference force.

(a)   (b)

Figure 50: Showing cup wall thinning effective by changing blank holder force **(a)** reference **(b)** decreasing blank holder force (20%) from reference force.
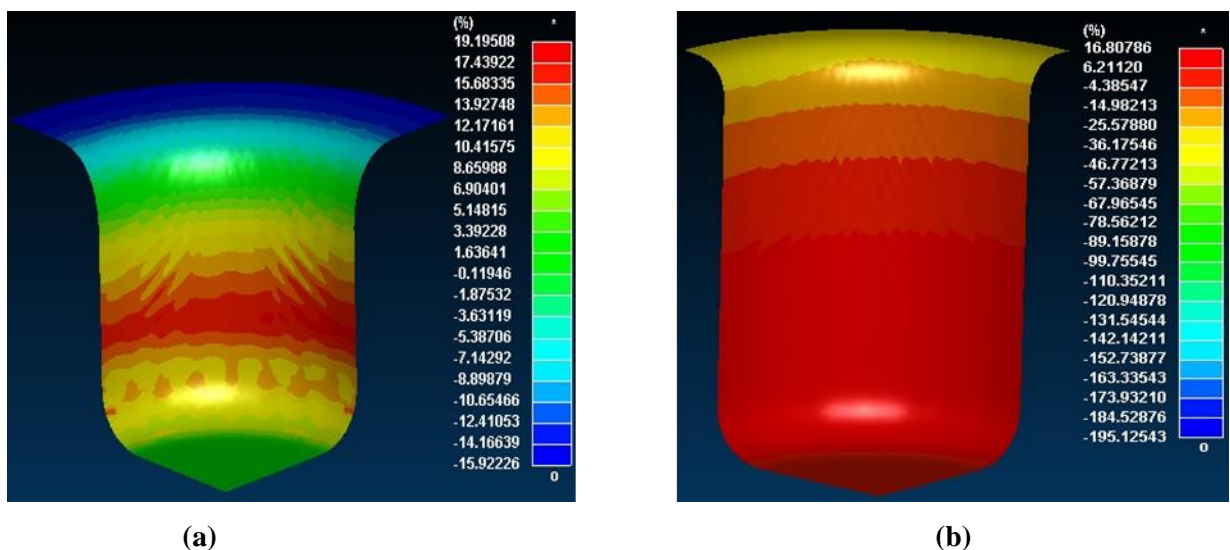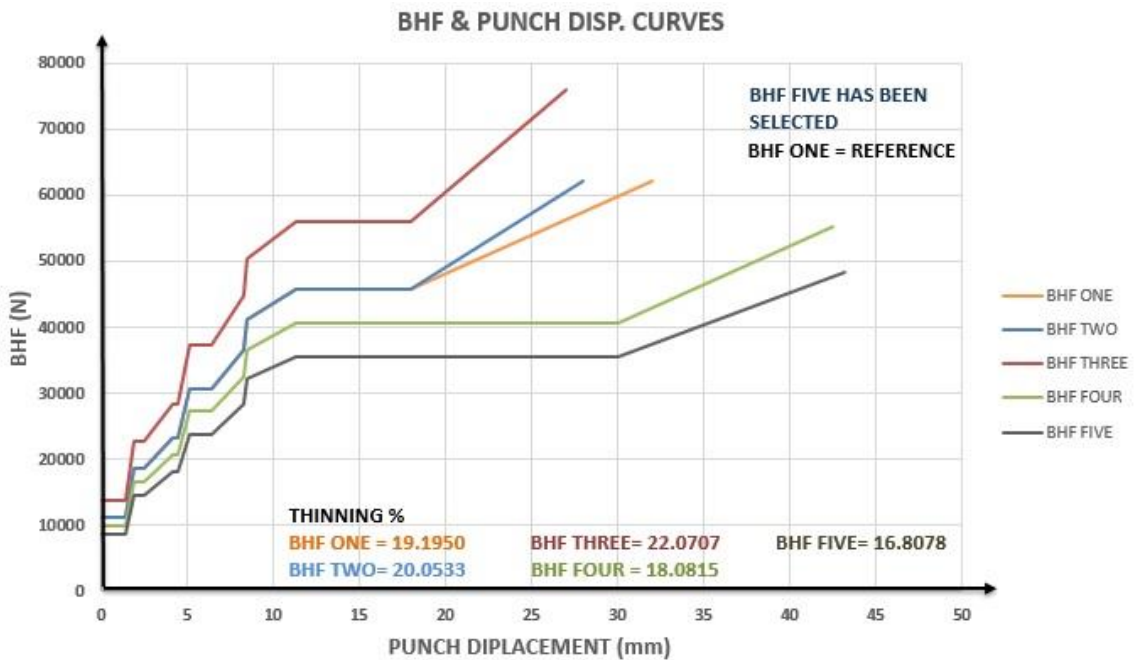
Figure 51: Showed BHF with Punch displacement curves with different values and results of thinning percentages of them.

5.3 Experimental Work Results

The parameters were obtained from the numerical study and installed on the PC to perform the experiment. The punch displacement, pressure path, and blank holder force were calculated experimentally in the lab.

5.3.1 Punch Displacement Value

To calculate the punch displacement in the lab, the blank is placed over the blank holder (Fig. 37), after which the punch is moved up freely until the blank touches die. At this moment, the value from the PC in the lab from the WIN-PED program is noted. In this experiment, the real value was 94 mm, which was added to the numerical values.

5.3.2 Pressure circle

The most important element that should be calculated before the other parameters is the pressure circle. In the simulation, it was calculated by calculating the diameter of the cavity in the die plus the diameter of the end of the radius in the blank holder (Fig. 52).

62

However, in the experimental work, we cannot do so as the pressure circle depends on the circle area which is a result from the calculated area of the die cavity plus the selected area above the drawing ring. In numerical study it was in the bar; however, in the experimental work, it was in the (Kgf).
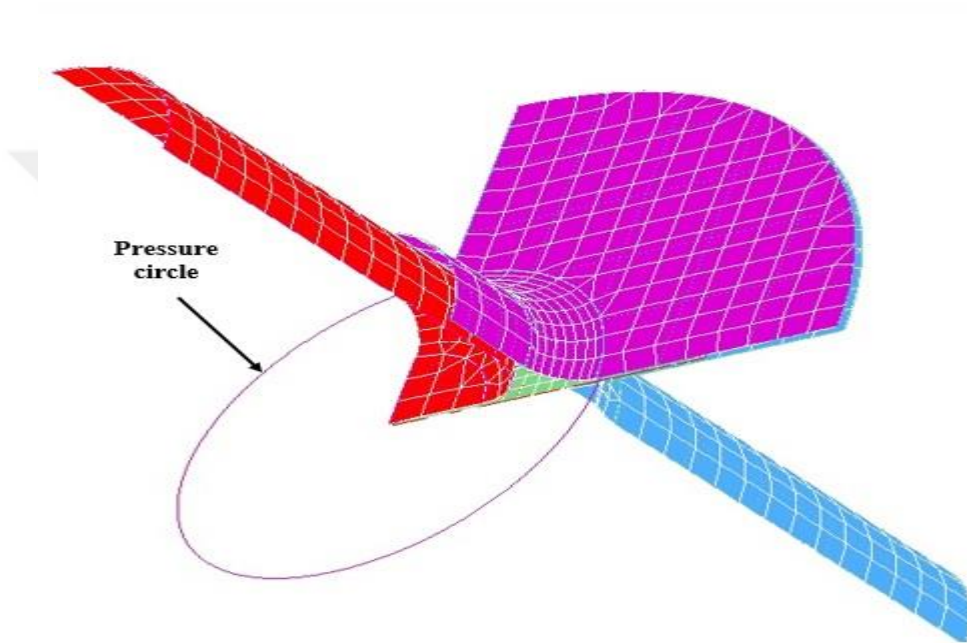

Figure 52: Pressure circle in numerical study (simulation).

5.3.3 Blank Holder Force

The blank holder force is other parameter that had to change. In the numerical study, it was calculated in MPa, which is the net blank holder force. However, this value cannot be used in the experimental work. In the experimental work, the blank holder force was derived from the blank holder force in the numerical study plus quantity chamber pressure multiplied by the calculated area. This is called the blank holder force experimental (BHF exp.). In this study, three values were trialed (Fig. 53), but the results of this experiment were not successful (Fig. 59 and Fig. 60).
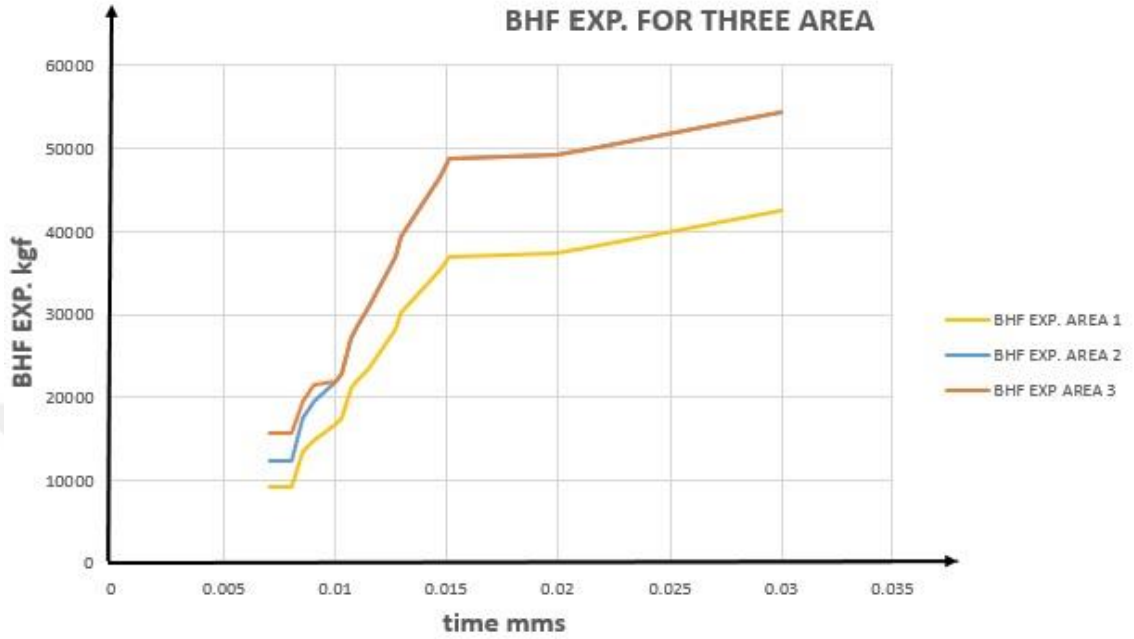
Figure 53: BHF Exp. Curves used in this study.
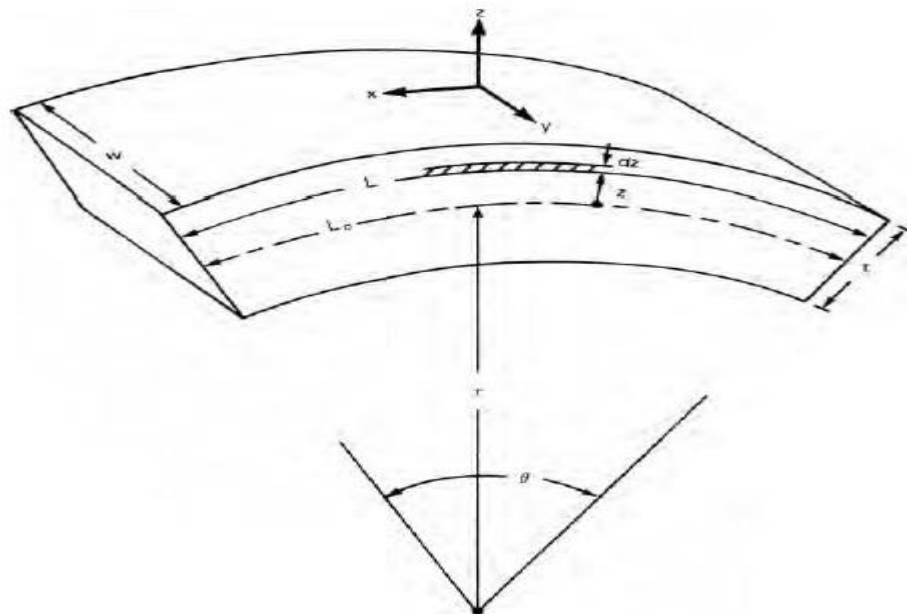
5.4 Sheet Bending Theory

Figure 54: Coordinate system for analyzing sheet bending.

After got bad results in first experimental work, failure reasons have been analyzed because of this analyzed, forming strain has been reduced by used sheet bending theory it is showing below (Fig. 54):

$$\epsilon_{\circ x} = \frac{L_1 - L_\circ}{L_\circ}$$

$$\because L_\circ = r * \theta \quad \text{And} \quad L = (r + z) * \theta$$

$$\therefore \epsilon_x = \frac{(r + z) * \theta - (r * \theta)}{(r * \theta)} \rightarrow = \frac{z}{r}$$

$$\epsilon_{x\,max.} \; when \; z = \frac{t}{2}$$

$$\therefore \epsilon_{x\,max.} = \frac{t}{2r}$$

If the   t = 1   and   r = 5

$$\epsilon_{x\,max.} = \frac{1}{2 * 5} = 0.1$$

Therefore, the inverse relationship between the radius of the formation and the maximum strain of the formation:

If   t = 1   and   r = 8

$$\epsilon_{x\,max.} = \frac{1}{2 * 8} = 0.0625$$

$$\therefore \epsilon_{r=8} < \epsilon_{r=5}$$

Therefore, the forming parameters re-calculated again with new tools dimensions (Fig. 55).
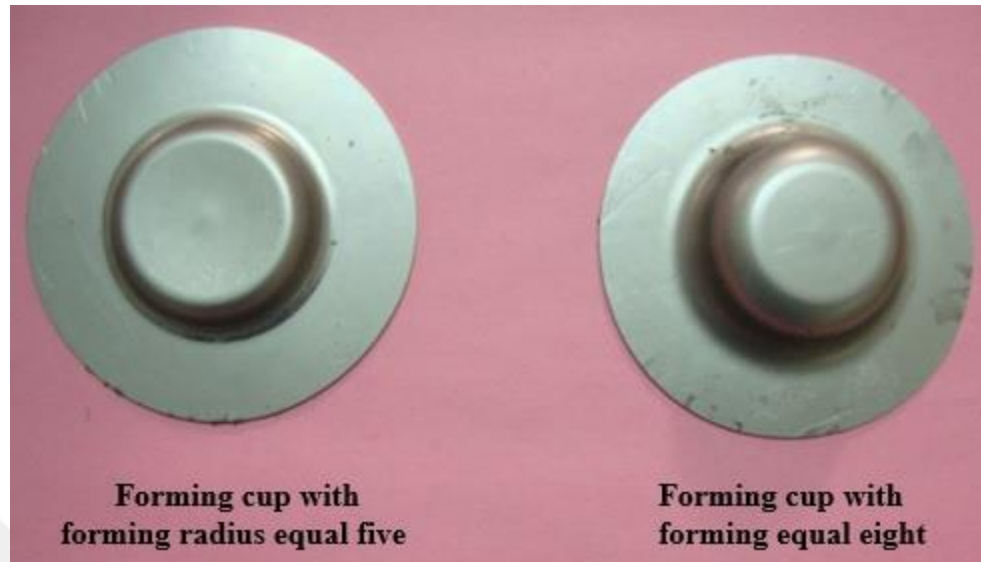
Figure 55: Cups with different forming radius.

5.5 Numerical Results for Second Study

The objective of the numerical study is to achieve the appropriate conditions for forming a Ti-6Al-4V alloy sheet. This study did so with a forming radius of $r_p = 8$ mm. After completing the analysis, the results were studied and classified.

5.5.1 Finite Element Simulations with Increased Blank Diameter

In this case, four attempts were made and for over 95 mm, all attempts were failures; therefore, 80 mm, 85 mm and 90 mm were selected. The simulation was started using an 80 mm diameter. Good results were calculated with a maximum wall thinning of 10.182% (Fig. 56). The second simulation was run using an 85 mm diameter. Good results were also obtained, with a maximum wall thinning of 9.989% (Fig. 57). The third attempt was an unsuccessful simulation with a 90 mm diameter; the maximum wall thinning was 20.491% (Fig. 58). The simulation results for the Ti-6Al-4V alloy sheet with the HHD process showed that the maximum diameter that can be formed equals 85 mm, meaning that the largest draw ratio is (2.2).
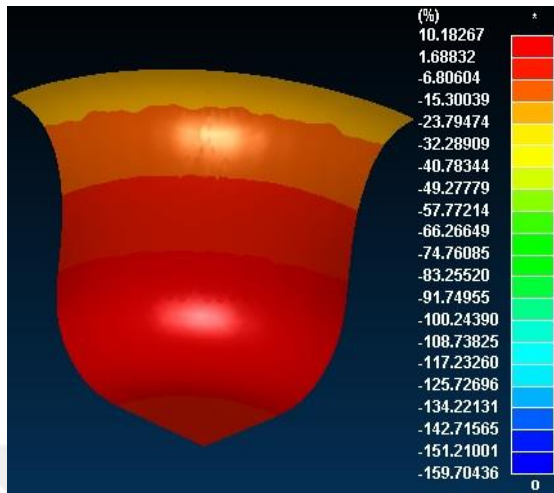
Figure 56: FEM of dia. =80 exp.2.   **Figure 57:** FEM of dia. =85 mm exp.2.
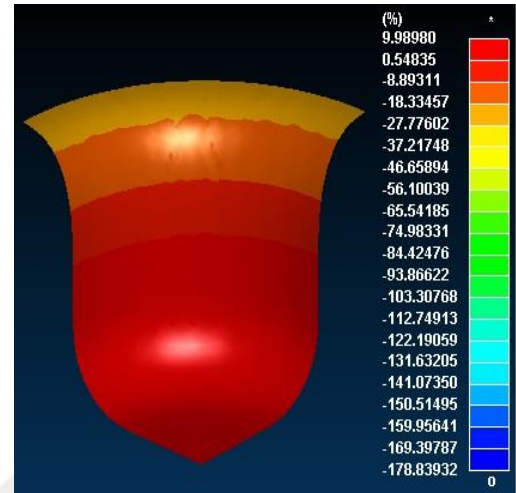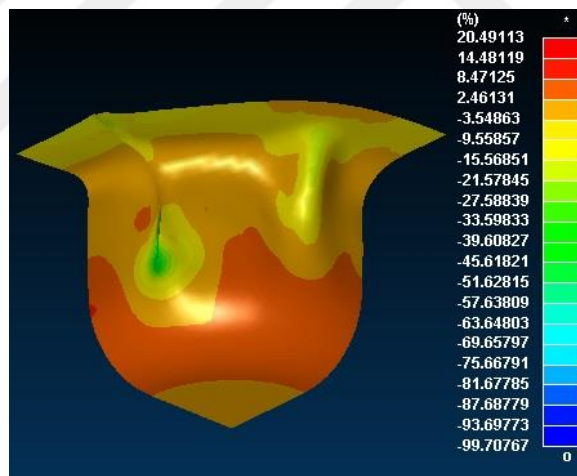
Figure 58: FEM of dia. =90 mm exp.2.

5.6 Forming Results for Experimental Work

As result of all these calculations, and after calculating and applying all parameters obtained from the numerical study, the alloy did not exhibit any formability (Fig. 56). These results were not similar to the numerical results, where the punch moved and touched the blank and fractured it. Moreover, changing the pressure area did not change anything in the results. After applying the bending theory, a change of tools (punch and

die) was carried out. Changing the forming radius for the punch and die from 5 mm to 8 mm to reduce forming was also carried out. The alloy exhibited different behavior such that it took more time to fracture (Fig. 57). Nevertheless, it was still a failure.

Figure 59: Ti-6Al-4V alloy blank after forming with fracture.

Figure 60: Ti-6Al-4V alloy blank after forming with fracture in second experimental.

5.7 Difference between Parameters in Experimental Work One and Two

After finished from two experiments. Drawing ratio, blank holder force, chamber pressure, and thinning percentage between two situations compared. Changed in forming radius led to reduce drawing ratio from (2.4) to (2.2), it is due to the friction area between punch and blank in experiment two is bigger than the experimental one. The second parameter effective by reduce forming radius is blank holder force, after changed forming radius for punch and die blank holder force; blank holder force was decrease (Fig. 61) . Pressure cavity is other parameter effective by reduced radius (Fig. 62) the pressure cavity in experiment one was higher than experiment two.
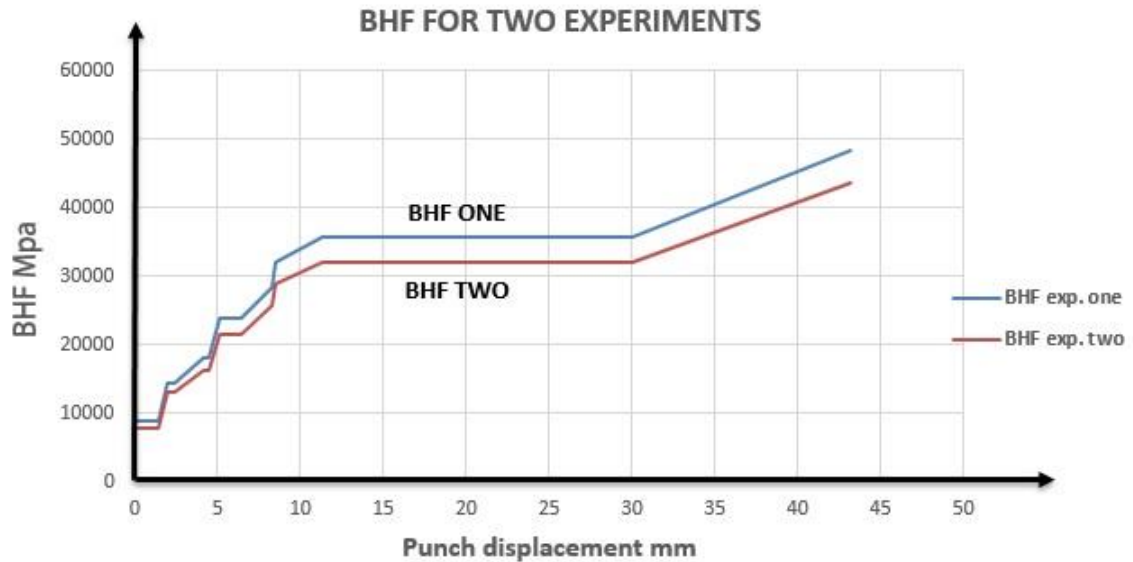
Figure 61: Comparing between blank holder force values for two experiments.
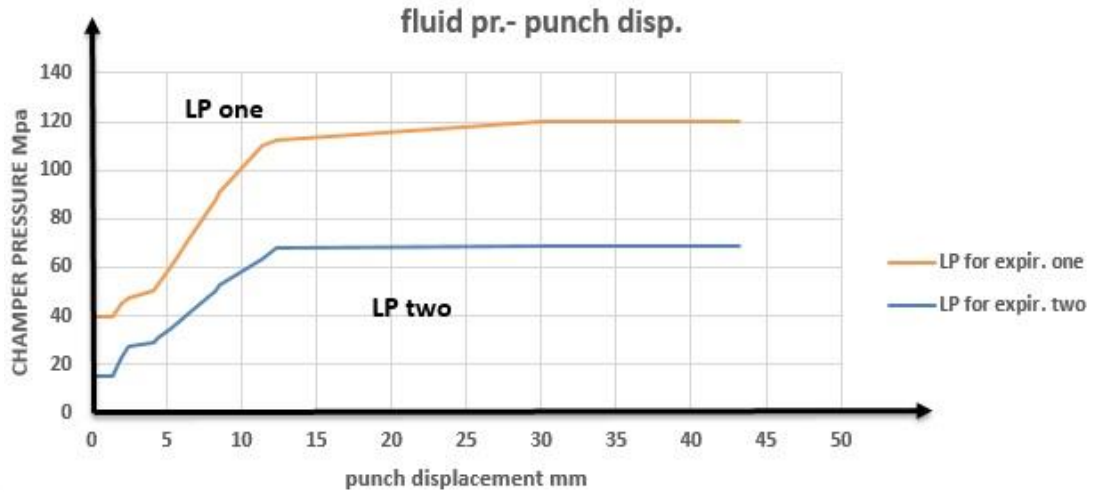
Figure 62: Comparing between chamber pressures for two experiments.

5.8 Stainless steel 304 experimental results

We have chosen stainless steel 304 with one mm thickness as a practical example to give credibility to the titanium alloy (Ti-6Al-4V) sheet experience. Because it has a good mechanical properties that increase its ability to form, For example, it has a good elongation, a good yield stress, and a good ultimate stress. In same boundary condition and tools; numerical and experimental study have been performed. In numerical study; 80 mm, 85 mm, and 95 mm were selected. The simulation was started with an 80 mm diameter. Good results were calculated and the maximum wall thinning percentage value was 8.46 % (Fig. 63). The second simulation used 85 mm, also with good results and maximum wall thinning percentage value of 9.25% (Fig. 64). The final simulation was performed with the 95 mm diameter, yielding a maximum wall thinning percentage value of 10.89% (Fig. 65). Simulation results for the stainless steel type 304 sheet in the HHD process showed that the maximum diameter can be equal to 95 mm, which means the largest draw ratio being reached is (2.4).
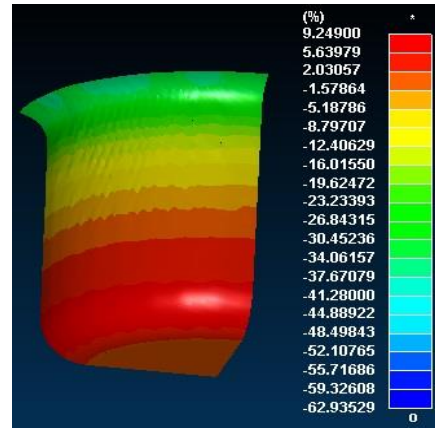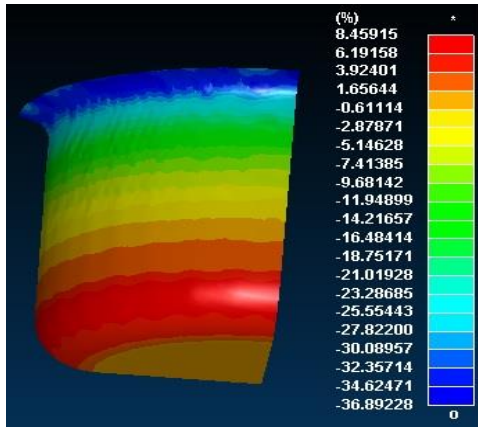
Figure 63 : FEM for St. Steel cup 304 with Dia. 80 mm **Figure 64** : FEM for St. Steel cup with Dia. 85 mm
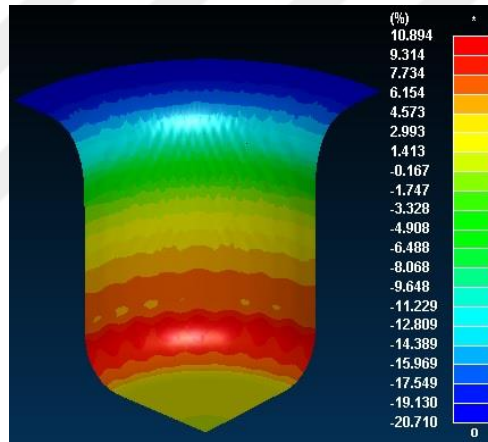
Figure 65 : FEM for St. Steel cup with Dia.95 mm.

After applying the ideal parameters obtained from the simulation in experiment the results showed that the numerical and experimental values were nearly identical (table. 9). The cups resulting from the forming process can be seen in (Fig. 67) the punch force required in experiment to form cups is illustrated below (Fig. 66)

Table 12 : Comparison between stainless steel 304 numerical and experimental parameters

Parameters	Numerical values	Experimental values
Diameter (D) mm	95	95
Punch force (N)	209196	248962
Fluid pressure (bar)	945	998
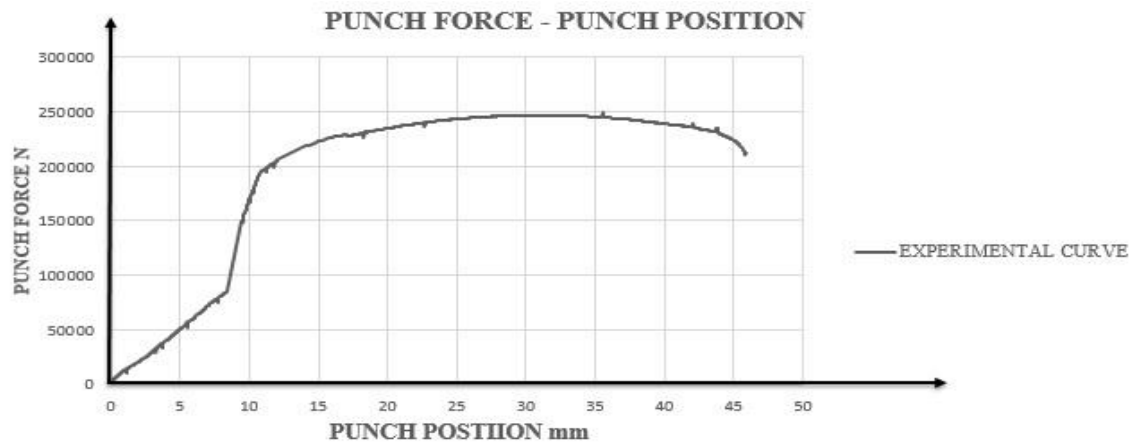
Figure 66 : relationship between punch force and punch position of stainless steel 304 experiment.

Figure 67 : Stainless Steel type (304) cups forming in same forming tools for (Ti-6Al-4V) sheet alloy.

5.9 Conclusion

This study is considered to be the first on hydro-mechanical deep drawing of Ti-6Al-4V sheet alloy. Using hydro-mechanical deep drawing to form Ti-6Al-4V sheet alloy was a great challenge due to Ti-6Al-4V sheet alloy having poor formability at room temperature and it has a high cost. Our investigation into Ti-6Al-4V sheet alloy formability by using hydro-mechanical deep drawing produced many points to be discussed. Tensile test, simulation, and experimental results were observed and conclusions were drawn. In the tensile test, the Ti-6Al-4V sheet alloy exhibited high values in its mechanical properties, such as an approximately 1150 MPa yield stress as well as ultimate stress and low formability with an elongation value of approximately 11%, but after the heat treatment values decreased. Due to alloy exhibiting a ductile behavior as its elongation value exceeded 5%, it was decided that the alloy should be formed with the HDD process at room temperature. In the numerical study, the forming of the alloy was investigated for two drawing radii (punch nose radii), namely 5 mm and 8 mm. Experiments were conducted for these two situations. The first experiment was performed with the 5 mm forming and die radii. The optimum fluid pressure and blank holder force paths' changing with the punch position were investigated for different sheet diameters, and it was trialed to determine the maximum blank diameter that could be successfully formed. As a result, forming could be achieved with 95 mm diameter blanks and a punch of 40 mm diameter. Therefore, the limiting drawing ratio that could be obtained was 2.4 through simulations of the process. However, the sheet was fractured at the start of the forming in the punch displacements of 2-3 mm. Therefore, it was not possible to form the blank using the same parameters in the experiments. It was concluded that the maximum bending strains caused tearing of the sheet with a punch nose radius of 5 mm. Therefore, it was increased to 8 mm. The optimal parameters were determined also for this radius. When the experiments were performed with new tools, the blank was formed more so than previously. Fractures occurred approximately at a 7 mm punch displacement, despite it having achieved producing a fully formed cup. It should be emphasized beforehand that in many studies conducted in the laboratory of Selçuk University, it has been shown in many published studies that there is a great consistency between experimental and numerical studies for aluminum and stainless steel materials.

However, in this study, it was found that there is an inconsistency between the numerical and experimental results for the Ti-6Al-4V titanium alloy. The mismatch between the numerical and experimental results may be due to a number of factors, such as the possibility of the material being highly sensitive to experimental uncertainties. The deviation from concentricity of the tools and the flatness of the blank holder can also affect the material. As the heat treatment had occurred in a normal furnace with oxygen availability, the alpha phase grew more than the beta phase, thereby possibly decreasing the formability. The third reason may be the material model being used. The material model may fail to predict the experimental results for titanium. It was concluded from the study that the simulations can predict material behavior successfully. For example, the St. Steel type (304) with 1 mm thick cups have been simulated and formed with the same tools under stainless steel boundary conditions. Consequently, it was concluded that while it is estimated that the material would be successfully formed with the optimum parameters determined in the simulations, it was found that these parameters did not give a successful forming result in the experimental work.

5.10 Future Work

The Ti-6Al-4 is an astounding alloy due to its properties and applications. Enhancing alloy sheet formability remains a good goal for further study. Therefore, the final point in this study can be taken as a starting point to other studies.

REFERENCES

[1] S. H. Zhang, J. Danckert Development of hydro – mechanical deep drawing, Journal of Materials Processing Technology 83 (1998) 14-25.

[2] Lihui Lang, Joachim Danckert, Karl Brian Nielsen Investigation into the effect Of pre-bulging during hydro-mechanical deep drawing with uniform pressure Onto the blank international Journal of machine Tool & Manufacture 44 (2004) 649-657.

[3] K. Nakamura, T. Nakagawa, Sheet Metal Forming with Hydraulic Counter Pressure in Japan. Annal. CIRP 36 (1987) 191-194.

[4] John, Jian-Feng Nie, Ma Qian"Light alloys book", David St.

[5] James K. Wessel**,** Wessel & Associates**,** Oak Ridge, Tennessee, "HANDBOOK OF ADVANCED MATERIALS ENABLING NEW DESIGNS "Copyright @ 2004 by John Wiley & Sons, Inc.

[6] Rafael Nunes **"**Properties and selection nonferrous alloys and special purpose material"s volume 2, the second printing (1992) by the ASM International Handbook Committee.

[7] J. Donachie, Jr. "Titanium a Technical Guide"*Second Edition* by Matthew ASM International® Materials Park, OH 44073-0002 www. asminternational.org.

[8] Lihui Lang*,* Tao Li A, Xianbin Zhou, Joachim Danckert, Karl Brian Nielsen "The effect of the key process parameters in the innovative hydroforming on the formed parts" Journal of Materials Processing Technology 187–188 (2007) 304-308.

[9] Lihui Lang, Joachim Danckert, Karl Brian Nielsen, Investigation into hydrodynamic deep drawing assisted by radial pressure, Part I. Experimental observations of the forming process of aluminum alloy, Journal of Materials Processing Technology 148 (2004) 119-131.

[10] Lihui Lang, Joachim Danckert, Karl Brian Nielsen. "Investigation into hydrodynamic deep drawing assisted by radial pressure Part II. Numerical analysis of the drawing mechanism and the process parameters" Journal of Materials Processing Technology 166 (2005) 150-161.

[11] Wei Liu, Yongchao Xu, Shijian Yuan "Effect of pre-bulging on wrinkling of curved surface part by hydro-mechanical deep drawing" 11th International Conference on Technology of Plasticity, ICTP 2014, 19-24 October 2014, Nagoya Congress Center, Nagoya, Japan. Procedia Engineering 81 (2014) 914-920.

[12] E. Cerettia, C. Giardinib, C. Contric and P. Bortotd, "Hydromechanical Deep Drawing Simulations: Model Development and Process Parameters Investigation" Advanced Materials Research, ISSN: 1662-8985, Vols. 6-8, pp. 353-360, Online: 2005-05-15.

[13] Liu Wanying, Lin Yuanhua, Chen Yuhai, Shi Taihe, Ambrish Singh. "Effect of Different Heat Treatments on Microstructure and Mechanical Properties of Ti6Al4V Titanium Alloy" Rare Metal Materials and Engineering**,** Volume 46, Issue 3, March 2017 Online English edition of the Chinese Language Journal.

[14] Ossama Mamdouh Badr, Bernard Rolfe, Peter Hodgson, Matthias Weiss, "Forming of high strength titanium sheet at room temperature" Materials and Design (2014).

[15] J. ADAMUS, P. LACKI "INVESTIGATION OF SHEET-TITANIUM FORMING WITH FLEXIBLE TOOL – EXPERIMENT AND SIMULATION" ARCHIVES OF METALLURGY AND MATERIALS, Volume 57 2012 Issue 4 DOI: 10. 2478/v10172-012-0139-8.

[16] Tuoyang Zhang, Yong Liu, Daniel G. Sanders, Bin Liu A, Weidong Zhang, Canxu Zhou "Development of fine-grain size titanium6 Al–4V alloy sheet material for low temperatures upper plastic forming" Materials Science & Engineering A, 608 (2014) 265-272.

[17] Aldo Corona, "Characterization of the Relationship between the Microstructure and Tensile Strength of Annealed Ti-6Al-4V", Senior Project Report June 2011.

[18] F. Djavanroodi,* A. Derogar" Experimental and numerical evaluation of forming limit diagram for Ti6Al4V titanium and Al6061-T6 aluminum alloys sheets" Materials and Design 31 (2010) 4866-4875.

[19] Nitin Kotkunde, Amit Kumar Gupta & Swadesh Kumar Singh, "Formability study of Ti-6Al-4V alloy under warm conditions" Advances in Materials and Processing Technologies, Formability study of Ti-6Al-4V alloy under warm conditions, Advances in Materials and Processing Technologies, 1:1-2, 210-222, DOI: 10. 1080 /2374068X. 2015.1118994.

[20] Zhiying Sun & Lihui Lang & Kui Li & Yao Wang & Quanda Zhang Study on the mechanism and the suppression method of wrinkling in side wall using hydroforming of the fairing.

[21] Muammer Koç, Hydroforming for advanced manufacturing book, Cambridge England,

[22] Shim, H., and Yang, D. Y., "A simple method to determine pressure curve for sheet hydro-forming and experimental verification", J. Mater. Process. Technol. Vol. 169, 2005, pp. 134-142.

[23] Morteza Alizad-Kamran, Mohammad Hoseinpour Gollo, Abbas Hashemi, S. M. Hossein Seyedkashi, Determination of critical pressure in analyzing of rupture instability for hydromechanical deep drawing using advanced yield criterion, archives of civil and mechanical engineering 18 (2018) 103-113.

[24] Lothar Wagner, "Status of titanium and titanium alloys in auto applications", Institute of Materials Sciences and Engineering, Clausthal University of Technology Germany. 23, Annual ITA conference and exhibition Orlando, FL, USA 7-9-2007.

[25] M. Tisza, "Numerical modelling and simulation in sheet metal forming", Faculty of Mechanical Engineering, University of Miskolc, Journal of Materials Processing Technology 151 (2004) 58-62.

[26] Nitin Kotkunde, Aditya D. Deole, Amit Kumar Gupta, Swadesh Kumar Singh, B. Aditya, "Failure and formability studies in warm deep drawing of Ti‑6Al‑4V alloy" Materials and Design 60 (2014) 540-547.

[27] Standard Test Methods for Tension Testing of Metallic Materials [Metric], Designation: E 8M – 04.

[28] Murat DELMEÇ, Mevlüt TÜRKÖZ, H. Selçuk HALKACI, "DESIGN OF STAMPING AND SHEET HYDROFORMING TEST UNIT" 12th International Research/Expert Conference "Trends in the Development of Machinery and Associated Technology" TMT 2008, Istanbul, Turkey, 26-30 August, 2008.

[29] Ekrem Öztürk, Mevlut Türkoz, Selçuk Halkacı, Mehmet Halkacı, An Application of Fuzzy Logic Control Algorithm in Hydro mechanical Deep Drawing Process Applied Mechanics and Materials Vol. 686 (2014) pp. 95-100.

[30] D Ravi Kumar, and M Manohar, "Determination of Process Parameters in Multi-Stage Hydro-mechanical Deep Drawing by FE Simulation" Materials Modelling and Testing for Sheet Metal Forming, IOP Conf. Series: Journal of Physics: Conf. Series **896** (2017) 012061.

[31] Takeshi Uemori and et al.,"Theoretical predictions of fracture and springback for high tensile strength steel sheets under stretch bending". International Conference on the Technology of Plasticity, ICTP 2017, 17-22 September 2017,Cambridge, United Kingdom. Procedia Engineering 207 (2017) 1594–1598.

[32] İ. ERKAN ÖNDER," ASSESSMENT OF SHEET METAL FORMING PROCESSES BY NUMERICAL EXPERIMENTS". A THESIS SUBMITTED TO THE GRADUATE SCHOOL OF NATURAL AND APPLIED SCIENCES OF MIDDLE EAST TECHNICAL UNIVERSITY.

[33] MILITARY HANDBOOK (MIL-HDBK-5H) 1 DECEMBER 1998, chapter five, page no. (5-1).

CURRICULUM VITAE

PERSONAL INFORMATION

Name, Surname	: Husam Al-KARAWI
Nationality	: Iraqi
Date and Place of Birth	: 14 June 1980, Iraq- Baghdad
Marital Status	: Married
Phone	: +90 5396870418
Email	: hassamkaese@yahoo.com

EDUCATION

Undergraduate	: University of Technology / Department of Production Engineering and Metallurgy, 2003.

WORK EXPERIENCE

Year	: 2004- Present
Place	: Ministry of Electricity

FOREIGN LANGUAGE

English